Prediction of Weight-on-Bit based on Real-Time Surface Measurements

Diploma Thesis

Author: Rainer Paulic

Mining University Leoben

Petroleum Engineering

Department for Drilling Engineering

Industry Advisor:

Dipl. Ing. Wolfgang Mathis

University Advisor:

Prof. Dr. Gerhard Thonhauser

Author: Rainer Paulic

Title: Prediction of Weight-on-Bit based on Real-Time Surface Measurements

Department: Mineral Resources & Petroleum Engineering – Drilling Engineering

Degree: M.Sc.

Year: 2007

Rainer Paulic, March 2007

Acknowledgement

The Author would like to thank the following:

Prof. Dr. G. Thonhauser – Managing Director of TDE GmbH, for his coaching and support

Dipl. Ing. W. Mathis – TDE GmbH, for his technical support

The staff from TDE GmbH, for their support, ideas and patience

Kurzfassung

Hohe Bohrfortschritte können nur mit der richtigen Meißellast erzielt werden. Diese zu kennen ist nicht nur für schnelleres Bohren von Wichtigkeit, sondern auch um hohe Standhaftigkeit von Bohrmeißel und Downhole Tools zu gewährleisten.

Heutzutage wird die Meißellast in den meisten Fällen mit einfachen Torque and Drag Modellen berechnet, welche fähig sind vernünftige Ergebnisse mit geringem Aufwand zu liefern. Andererseits gibt es gewisse Zustände während des Bohrens, welche mit diesen Modellen nicht simuliert werden können. Stick-Slip ist einer dieser Zustände, die mit herkömmlichen Methoden nicht modelliert werden können. Feder-Masse Modelle sind jedoch fähig, diese Zustände zu modellieren. Außerdem kann man mit Feder-Masse Modellen auch die Veränderungen der Länge des Bohrstranges berechnen. Aus diesem Grund sind mit solchen Modellen genauere Ergebnisse zu erzielen. Wenn diese Modelle einfach gehalten werden, sind sie in der Lage bessere Ergebnisse zu liefern, ohne die Leistung der Computer zu sehr zu belasten.

Das Ziel dieser Arbeit war es ein alternatives Modell zu den momentan gebräuchlichen Modellen vorzuschlagen. Da dieses Modell in Echtzeit laufen sollte, darf es nicht zu kompliziert werden, sollte aber nichtsdestotrotz genauere Ergebnisse als herkömmliche Modelle liefern. Außerdem sollte das Modell fähig sein gewisse Bohrzustände zu modellieren, die die Kraftübertragung durch das Bohrgestänge beeinflussen. Um diese Zustände jedoch behandeln zu können, müssen diese erst erkannt werden.

Mittels zwei Datensets, eines mit Messungen, die an der Oberfläche gemacht wurden, und eines mit Messwerten eines Downhole Tools, wurden verschiedene Methoden zur Erkennung dieser Fehlzustände beim Bohren untersucht. Während Buckling des Bohrstranges mit herkömmlichen Methoden zu ermitteln ist, muss für Stick-Slip nach einer anderen Methode gesucht werden.

Stick-Slip ist ein Bohrzustand, bei dem der Bohrstrang abwechselnd in Ruhe und in Bewegung ist. Während der so genannten Sticking Phase, in der der Bohrstrang in Ruhe ist, kommt die Kraftübertragung zum Meißel zum Erliegen, da die Haftreibung höher ist als die Gleitreibung bei einem rotierenden Bohrstrang. Jeder weitere Versuch Kraft auf den Meißel zu bringen wird nur die potentielle Energie des Bohrstranges erhöhen, ähnlich einer Feder die zusammengedrückt wird. Nachdem genügend Drehmoment aufgebaut wurde, um die Haftreibung zu überwinden und den Bohrstrang wieder in Bewegung zu setzen, rotiert dieser für kurze Zeit mit viel höheren Drehzahlen als dies normalerweise der Fall ist. Dadurch nähert sich die axiale Gelitreibung gegen null, und die aufgestaute potentielle Energie wird frei. Diese

unkontrollierte Kraftübertragung kann zu extrem hohen Meißellasten führen und sehr schädlich für jegliches Downhole Equipment sein.

Eine Methode um Festzustellen ob sich Stick-Slip Bedingungen gebildet haben wurde im Zuge der Arbeit untersucht. Mittels der Drehzahl des Meißels als Eingabeparameter kann ein Stick-Slip Index berechnet werden, mit welchem man vorhersagen kann, ob sich Stick-Slip Bedingungen gebildet haben oder nicht. Diese Vorhersage kann dann wiederum vom Feder-Masse System übernommen werden.

Ein anderer wichtiger Aspekt dieser Arbeit war die Bestimmung der Reibungskoeffizienten für das Bohrloch. Der Einsatz eines Feder-Masse Modells macht nur Sinn, wenn die Reibungskoeffizienten über das ganze Bohrloch hinweg bekannt sind. Ein MATLAB Programm ist fähig einen Reibungskoeffizienten während des Ausbauens des Bohrstranges zu berechnen. Indem man diese Berechnung in kleinen Abschnitten durchführt, ist es möglich für jeden Abschnitt des Bohrloches einen Reibungskoeffizienten zu ermitteln.

In naher Zukunft werden die Berechnungen durch neuronale Netzwerke gelöst werden, welche weniger Ressourcen brauchen als herkömmliche Programme. Aus diesem Grund wären neuronale Netzwerke die beste Lösung für Echtzeitanwendungen. Andererseits liefern neuronale Netzwerke nur dann brauchbare Ergebnisse, wenn sie an die an bestimmte Bedingungen angepasst werden („Training“). Parameter, die den Trainingsbereich der neuronalen Netzwerke überschreiten, können zu falschen Ergebnissen führen. In so einem Fall könnte man auf Feder-Masse Modelle zurückgreifen, um Parameter zu berechnen, die wiederum für das Training von neuronalen Netzwerken benutzt werden können.

Abstract

High rates of penetration during drilling operations can only be achieved when using the right weight-on-bit. Knowing the weight-on-bit is not only of importance for faster drilling, but also in order to ensure a high lifetime of the drilling bit and the downhole equipment.

Currently the weight-on-bit is in most cases estimated by using simple torque and drag models. These models are able to deliver reasonable results with minimum computer performance consumption. However, there are certain drilling conditions which can not be modelled by these simple torque and drag models. Stick-slip is one of these drilling conditions which can not be modelled using such calculations. Spring-mass models are capable of modelling more different drilling conditions, including stick-slip. Furthermore spring-mass models take the dimensional changes of the drillstring into account, hence enabling more exact results. If kept simple, spring-mass models can model the behaviour of the drillstring without being too demanding regarding computer performance.

It was the scope of this thesis to suggest an alternative model to the models that are currently in use. The model should be able to run in real-time, which meant that it should not be too complex, but be able to deliver better results than the models that are commonly used. The model should also be capable to handle different drilling dysfunctions which influence the axial force transfer to the bit. In order to handle these drilling dysfunctions the program has to be able to detect them.

Using two data sets, one with data measured at the surface and one set with measurements from a downhole tool, methods to detect drilling dysfunctions have been investigated. While drillpipe buckling can be detected using the common approach of finding the critical buckling loads, a different solution had to be found to detect stick-slip.

Stick-slip is a drilling condition where the drillstring is alternately in motion and at rest. While it is at rest, during the so called sticking phase, the axial force transfer might come to a halt because the static friction is considerably higher than the kinetic one. Any further slack-off of weight will not result in a higher weight-on-bit, but only in a higher potential energy of the drillstring, similar to the potential energy stored in a compressed spring. Once enough torque has been built up to overcome the static friction, the drillstring will rotate at much higher rotational speed than it normally should. As a consequence, the axial friction will nearly equal zero, resulting in a sudden release of potential energy. The uncontrolled axial force transfer might result in extremely high weight-on-bit and may be very damaging to the bit as well as to the downhole equipment.

A method to determine whether stick-slip conditions have set in has been investigated. Using the bit rotations per minute as input a so called stick-slip index can be calculated. This stick-

slip index can be used to forecast if there is stick-slip or not. This can then be used as an input for the spring-mass model.

Another important aspect of the work was the determination of the friction factors for the wellbore. Using a spring-mass model only makes sense if the friction factors are known over the whole length of the wellbore. A MATLAB application, which is capable to calculate a wellbore friction factor during pulling out of the hole, has been set up. If done not over the whole wellbore, but in incremental steps, the program is capable of calculating the friction factor for each part of the wellbore.

In the near future all the calculations may be done by neural networks. These offer the advantage of delivering results with a minimum consumption of computer performance. Therefore neural networks might be the best solution for real-time applications. On the other hand, neural networks can only be used when they had been well trained to certain conditions. If the drilling conditions exceed the parameters they had been trained to, the results might be totally wrong. In such a case spring-mass models may be quite useful to calculate input data for neural network training.

Table of Contents

List of Figures

Introduction

Axial force transfer from the surface down to the bit is commonly modelled using softstring torque and drag models. These models have the advantage that they are simple to use and easy to program. They do not require very much computer performance, so that they can even be used in real-time mode. On the other hand these models have some disadvantages. Common torque and drag models do not account for dimensional changes of the drillstring. Since certain drilling situations can only be modelled using a model that takes the dimensional changes into account, the results of the softstring torque and drag models may not be correct in these situations.

The problem can be solved using spring-mass models. These models have great advantages over common torque and drag models, because they are capable of taking the dimensional changes of the drillstring into account. The drillstring is not a rigid system, but it is subject to changes in length due to different forces acting on it. The axial main force that is acting on the drillstring during the drilling process, but also during tripping operations, is the frictional force. The effect of friction on the drillstring can be modelled to a reasonable extend by using mass-spring models.

When it comes to drilling dysfunctions, a mass-spring model has even bigger advantages over the standard torque and drag model. The effects of stick-slip, a well investigated drilling dysfunction, can be modelled using this kind of drillstring model. During stick-slip the drillstring is alternately in motion and at rest, changing its status every few seconds. While the drillstring is at rest, axial force transfer comes to a standstill, because the static friction is much higher than the kinetic one. After sufficient torque had been built up to free the drillstring again, the drillstring is rotating at much higher rotating speeds than it normally does, resulting in an axial friction factor which nearly equals zero. At this moment the axial force will be transferred down to the bit in a rather uncontrolled manner. Using the dependency of the axial friction factor on the rotating speed of the drillstring and taking the potential energy of the drillstring after the sticking phase during stick-slip into account, the spring-mass model is capable of modelling the effects of stick-slip.

Another drilling dysfunction that changes the dimensions of the drillstring is the buckling of the drillpipe. If the drillpipe is under compression, it will tend to buckle. Buckling will change the apparent length of the drillpipes. More importantly, buckling will induce additional contact forces between the drillpipe and the borehole wall. These contact forces will create additional frictional forces, which, as an effect, will worsen the problem with buckling. Once buckling is in helical mode and the frictional resistance is high enough to prevent axial force transfer, the drillpipe is in a lock-up condition. This means that force transfer down the drillpipe is not possible any more, but will only lead to a more and more buckled drillpipe.

Spring-Mass Model

Reasons to use Spring-Mass Models

Spring-mass models are an alternative way of modelling the behaviour of a drillstring. Using a set of springs and masses, which describe the different parts of the drillstring, may offer many advantages over the simple torque and drag models. The different properties of the drillpipe, like stiffness or length, can be incorporated into the properties of the spring. The mass of the spring-mass model is used to simulate the weight of the drillpipes and all the effects that are related to the weight of the drillpipe, like stretch of the drillpipe due to weight, tension in the drillpipes as well as normal forces between the drillpipe and the borehole wall due to gravity.

Basic Design

A spring-mass model consists of a set of springs which are connected with masses. The springs may have different properties, which are used to model the behaviour of the system. The masses are reduced to single points, so they have no spatial dimensions. The spatial dimensions of the system are modelled using the springs. If modelling a drillstring, for example, the spring is used to model the length of the drillstring, as well as its mechanical properties. The mass is located at the lower end of the spring and used to reflect the weight of the drillstring. An inclination value of the wellbore corresponds to each of these masses. Therefore the normal force between the wellbore and the mass (representing one part of the drillstring) can be calculated, enabling torque and drag analysis.

During the drilling process the drillstring is subject to many external forces. The weight of the drillpipe itself will cause the drillstring to elongate. Friction forces related with tripping operations will also elongate the drillstring (when pulling out of the hole), or contract it (when running into the hole). Changes in temperature influence the dimensions of the drillstring. Furthermore, pressure differences between the inner part of the pipe and its annulus might also have influences on the dimensions of the pipe. In order to model all of these effects, they have to be clearly understood, so that they might get incorporated into the spring-mass model. The next paragraphs describe the influences of these external forces.

Stretch of the Drillstring due to applied Force

Force applied to a body of a certain ductile material results in an elongation of the body to which the force is applied. If the force applied to the body does not exceed a certain value, the so called yield strength, the body will return into its original shape after the force is being released again. The relationship between stress (force per area) and strain (elongation of the body) up to that point is nearly linear. After reaching the yield strength of the material, the stress-strain curve flattens a little bit. Further deformation will result in an increase in stress, as the material reaches its strain hardening region. The highest point of the stress-strain curve is called the ultimate stress of the material. Any further deformation will result in a rupture of the specimen.

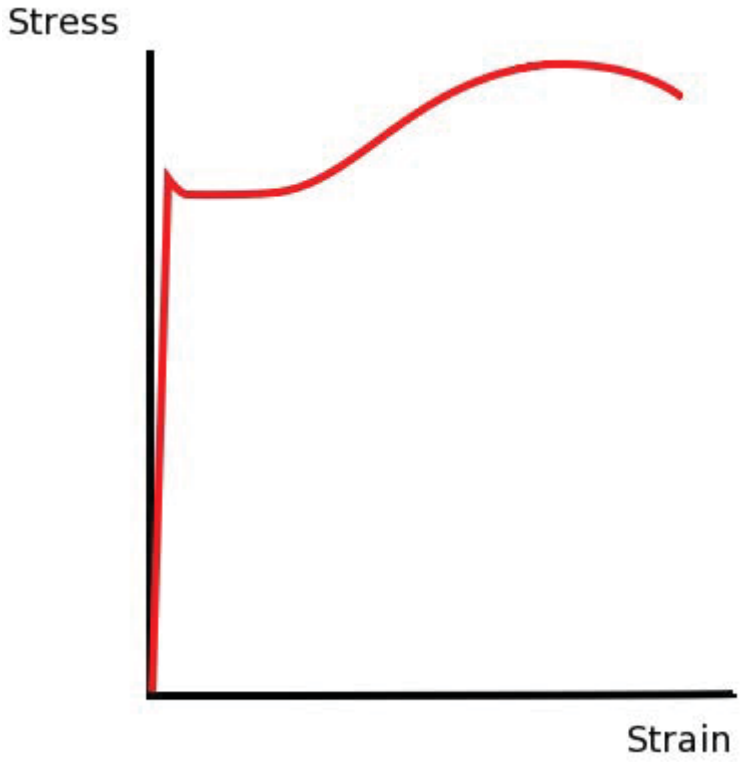

Figure 1 - Stress-Strain Diagram

For most engineering purposes only the part of the curve up to the yield strength is of importance. This part is also called elastic region of a material. The nearly linear relationship between stress and strain in that region can be modelled by Hooke's law:

$$\sigma = \frac{F}{A} \qquad \text{Eq. 1}$$

$$\varepsilon = \frac{\Delta l}{l}$$ Eq. 2

$$\sigma = E \cdot \varepsilon$$ Eq. 3

σ..... Strain [N/m^2]
F…… Force [N]
A…… Area [m^2]
ε……... Strain [ ]
Δl…….. Change in length [m]
l……. Length [m]
E…….. Modulus of elasticity / Young's modulus [N/m^2]

E is the constant of proportionality in Hooke's Law and is called modulus of elasticity (also called Young's modulus). When plotting the stress of a body against its strain, the modulus of elasticity can be determined by the slope of the curve in the elastic region. The value of Young's modulus for steel is 190 – 210 * 10^9 [Pa] or 30 * 10^6 [psi].

Using Hooke's law, the elongation of a certain body, which is subject to a certain force, can be calculated.

$$\frac{F}{A} = E \cdot \frac{\Delta l}{l}$$ Eq. 4

Rearrangement of the equation leads to:

$$\Delta l = \frac{1}{E} \cdot l \cdot \frac{F}{A}$$ Eq. 5

Another common form of writing Hooke's law is the spring equation.

$$F = -k \cdot x$$ Eq. 6

F……...Force [N]

k……Spring constant [N/m]

x……Stretch of the spring [m]

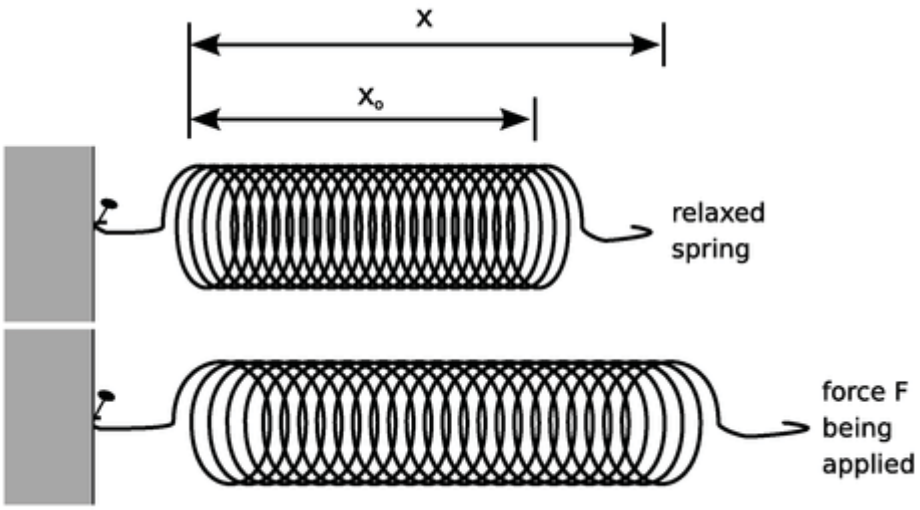

Figure 2 - Streched Spring

The negative sign in this equation indicates that the force exerted by the spring is in opposite direction than the direction of displacement. The spring constant k is the factor of proportionality between the force F exerted by the spring and the displacement x of the end of the spring. The unit of the spring constant is measured in [N/m].

The deformed spring is able to store potential energy. The potential energy stored in a spring can be calculated by integration of the spring equation over the displacement:

$$dE_{pot} = -F\ dx = -(-k \cdot x)dx = k \cdot x\ dx \qquad \text{Eq. 7}$$

$$E_{pot} = \int_0^x k \cdot x\ dx = \frac{1}{2}kx^2 + E_{pot,0} \qquad \text{Eq. 8}$$

E_{pot}…. Potential energy [J]

$E_{pot,0}$ is the potential energy of the spring at x = 0 when the spring is in state of equilibrium. If we set $E_{pot,0}$ = 0 the equation above reduces to

$$E_{pot} = \frac{1}{2} k x^2 \qquad \text{Eq. 9}$$

When setting up a mass-spring model to simulate the behaviour of a drillstring, the spring equation will be the basic equation. If the drillstring is at rest, then the buoyant gravitational force of the drillstring due to its weight will be the only force acting on the spring. Once the drillstring is moved, additional forces acting on the mass will influence the resultant force. These additional forces are frictional forces or the weight-on-bit during drilling operations.

Elongation / Contraction of the Drillstring due to Changes in Temperature

Basically every material changes its dimensions when it is exposed to different temperatures. Changes in temperature force the material either to expand (when an increase in temperature is observed) or to contract (for a decrease in temperature).

The elongation or contraction of a body can be obtained from the following equation:

$$\Delta l = \alpha \cdot l \cdot \Delta T \qquad \text{Eq.10}$$

Δl……..Change in length [m]
l…….Length [m]
α……Thermal expansion coefficient [K^{-1}]
ΔT…….Change in temperature [K]

The constant of proportionality in this equation is called linear thermal expansion coefficient. Strictly regarded, the linear thermal expansion coefficient is dependent on temperature, but for engineering purposes it can be regarded as a constant even for larger temperature spans.

Listed below there are typical values of the thermal expansion coefficient for different types of steel:

Material	Thermal Expansion Coefficient in [K^{-1}] at 20°C
Stainless steel	$17.3 * 10^{-6}$
Carbon steel	$10.6 * 10^{-6}$
Iron or Steel	$12 * 10^{-6}$

Table 1

Pressure Differentials

The paper of Paslay et al.[1] describes the influence of different pressures in the drillpipe and in the annulus on the tension in the drillpipe. The relationship between true tension in the drillpipe and effective tension is given by the following equation:

$$F_{t,eff} = F_{t,true} - p_i A_i + p_o A_o \qquad \text{Eq. 11}$$

For the sake of simplicity it is assumed for most toque and drag calculations that the pressure inside the drillpipe is equal to the pressure in the annulus. In this case the equation above simplifies to:

$$F_{t,eff} = F_{t,true} - pA_i + pA_o = F_{t,true} + p\left(A_o - A_i\right) = F_{t,true} + pA_{cs} \qquad \text{Eq. 12}$$

The true tension in the drillpipe can therefore be calculated as follows, assuming same pressures inside and outside the pipe:

$$F_{t,true} = F_{t,eff} - pA_{cs} \qquad \text{Eq. 13}$$

This equation shows the concept of buoyancy: The effective tension of the drillpipe is reduced by the force which the fluid pressure exerts to the drillpipe, resulting in the true tension of the pipe. Using this true tension, the axial stress in the drillpipe can be calculated as follows:

$$\sigma_{ax} = \frac{F_{t,true}}{A_o - A_i} = \frac{F_{t,true}}{A_{cs}} \qquad \text{Eq. 14}$$

$F_{t,eff}$.....Effective tension [N]
$F_{t,true}$.... True tension [N]
A_i..... Area enclosed by inner diameter of the drillpipe [m^2]
A_o..... Area enclosed by outer diameter of the drillpipe [m^2]
A_{cs}..... Cross-sectional area [m^2]
p_i.....Pressure inside the drillpipe [Pa]
p_o..... Pressure outside the drillpipe [Pa]
p..... Pressure [Pa]
σ_{ax}..... Axial stress [N/m^2]

Converting a Drillstring into a Spring-Mass Model

In order to use a spring-mass model to simulate the behaviour of the drillstring, the properties of the drillstring have to be incorporated into the spring-mass model. Several sets of springs and masses are used to represent the whole drillstring. Since the drillstring itself may consist of several sections, like bottom-hole assembly, heavy-weight drillpipes and normal drillpipes, the springs and masses may also have different properties. Springs which represent the behaviour of drill collars have a greater stiffness than springs representing drillpipes. The masses of the different sections might also be different, according to the weight of the pipes.

Springs

The springs of the spring-mass model should represent the mechanical properties of the drillstring, as well as the length of one segment of undeformed drillpipe.

The mechanical properties of the drillipipe are represented by the spring constant. By combining equations 4 and 6 the following relationship can be obtained:

$$F = E \cdot A \cdot \frac{\Delta l}{l} = k \cdot x \qquad \text{Eq. 15}$$

Since the elongation of the specimen is equal to the change in length of the deformed spring, the equation can also be written like this:

$$E \cdot A \cdot \frac{\Delta l}{l} = k \cdot \Delta l \qquad \text{Eq. 16}$$

The changes in length for the specimen and for the spring cancel. Rearrangement leads to:

$$k = E \cdot \frac{A}{l} \qquad \text{Eq. 17}$$

F……...Force [N]
k……Spring constant [N/m]
E……...Modulus of elasticity / Young's modulus [N/m^2]
A…….. Area [m^2]
l…….Length [m]
Δl……..Change in length [m]
x……Change in length of the spring [m]

The length of the spring should be equal to the length of the undeformed drillstring segment it represents.

Masses

The masses of the spring-mass model are used to represent the weight of each drillstring segment. The mass of one single mass can be calculated by multiplying the buoyed weight of the drillstring per unit length times the length of the drillstring segment.

$$m = w \cdot l_{segment} \qquad \text{Eq. 18}$$

m…….. Mass [kg]
w…….. Weight per Length of the drillstring [kg/m]
$l_{segment}$.. Length of the drillstring segment [m]

Note that all special dimensions are incorporated into the spring. The mass is reduced to a single point without special dimensions. All the friction calculations can be done nevertheless, because the frictional force is independent of the contact area, but only on the normal force.

Behaviour of the Spring-Mass Model

A spring-mass model offers great advantages over other common torque and drag model because of its ability to take dimensional changes of the drillstring into account. Each movement of the drillstring is related with friction. The frictional force acts against the direction of the movement and might increase or decrease the hookload by increasing or decreasing the tension in the drillpipes. Friction will also increase the resistance against rotation and therefore the torque needed to rotate the drillstring.

When using a spring-mass model, the drillstring may consist of several springs and masses.

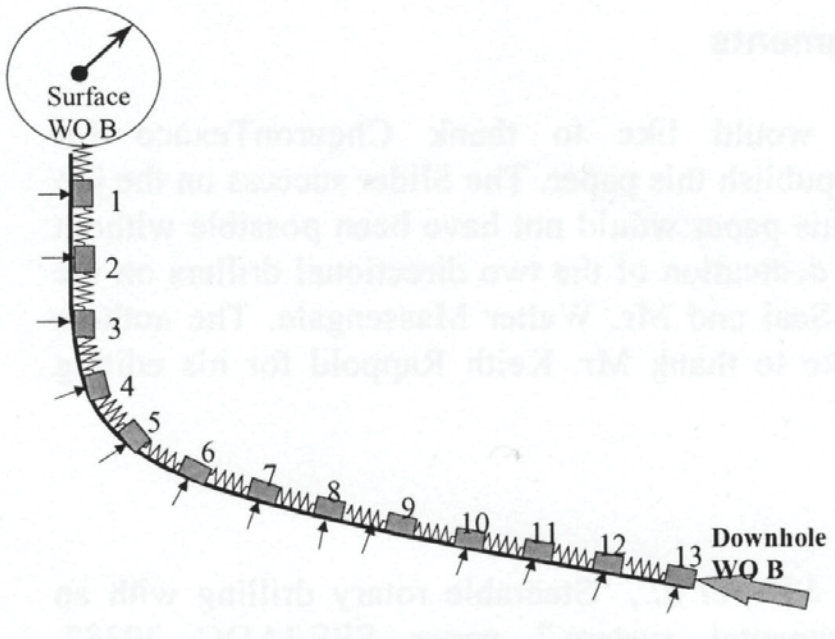

Figure 3 - Spring-Mass Model of a Drillstring

Behaviour without Rotation of the Drillstring

First the special case of a pure sliding motion of the drillstring will be investigated. In this case all the friction resists the axial movement of the pipe.

Any slack-off in weight at the surface will cause more and more masses to overcome the static friction and move. In the meanwhile the springs get compressed by the fictional force acting against the movement of the masses. Potential energy will be stored in the compressed springs. Furthermore the total length of the drillstring will be reduced due to the compression.

If the drillpipe is being picked up, the frictional force will cause the drillstring to stretch. Again, only the first masses will overcome the static friction at the beginning. After being picked up sufficiently, all the masses of the drillstring will have overcome the static friction and will move. Just like in the first case of lowering the drillpipe into the well, potential energy will be saved in the springs that make up the drillstring.

Description of an Application to Simulate the Behaviour of a Spring-Mass Model

A program can be set up using MATLAB: The movement of the block will compress the first spring of the spring-mass model. If the force exerted by the compressed spring is high enough to overcome the static friction of the fist mass, then the friction will change to kinetic friction. This kinetic friction will act against the first mass and contribute to the overall compression of the drillstring. The first mass will have the same displacement as the block, minus the length change due to compression of the spring. Therefore the second spring is not able to exert as much force onto its mass as the first spring. By using a loop over all of the springs and the masses, the displacement for every mass can be calculated, as well as the dimensional changes of the springs.

This program does not take transient effects of the springs and the masses into account. Once the static friction has been overcome by building up sufficient force, the mass will get accelerated by the resulting force which is acting on the mass. The resulting force is the force of the spring minus the dynamic frictional force:

$$F = F_{spring} - F_k \qquad \text{Eq. 19}$$

$$F = m \cdot a \quad \Rightarrow \quad a = \frac{F}{m} \qquad \text{Eq. 20}$$

F……... Force [N]
F_{spring}… Force exerted by the spring [N]
F_k……. Kinetic friction [N]
m…….. Mass [kg]
a…….. Acceleration [m/s^2]

Once the mass is being accelerated, the spring gets less and less compressed, hence exerting less and less force onto the mass. After a sufficient time, the acceleration of the mass equals zero and the mass will move with the same speed as the block. This transient acceleration effects are neglected in the model described above. It is assumed that the transition period is very short and that the mass is moving with the same velocity as the block.

Behaviour with Rotation of the Drillstring

In case of a rotating drillstring, the axial friction resisting the movement of the drillstring will be much less than in case of a non-rotating drillstring. The relationship between axial friction and rotating speed of the drillstring is given by the following equation:

$$\mu_{ax} = \mu \cdot \sin\left(\arctan\frac{v_x}{v_y}\right) \qquad \text{Eq. 21}$$

For a rotating pipe the following equation is valid:

$$v_x = \frac{\pi \cdot D \cdot n}{60} \qquad \text{Eq. 22}$$

v_x…….. Axial moving speed [m/s]
v_y…….. Tangential moving speed [m/s]
μ…….. Friction factor [ ]
$\mu_{ax.}$…… Axial friction factor [ ]
D…….. Outer diameter of the pipe [m]
n…….. Rotating speed of the pipe [rpm]

Since the axial friction is much reduced in case of a rotating drillstring, the whole drillstring will be easier to move. Furthermore, the dimensional changes of the drillstring are also reduced, and, by effect, the potential energy stored in the deformed drillstring.

Special Cases

In case of stick-slip, where the drillstring is alternately at rest and in motion, any slack-off during the sticking phase will result in an increase potential energy of the springs simulating the drillstring. Once the drillpipe starts rotating again, the axial friction will get close to zero, resulting in a sudden release of potential energy.

Common Torque and Drag Models

In order to simulate the behaviour of the drillstring several torque and drag models are in use. The complexity of these models range from simple torque and drag calculations up to very complex drillstring modelling using the finite elements method. The scope of this thesis is to propose a model which should deliver reasonable results without being too complex, so that it could be run in realtime. The more complex a model gets, the more time it takes to get a result. Therefore all models which take too much calculation time are not useful for these real-time applications. The model should nevertheless be able to take several aspects of the dynamics of the drillstring into account.

Softstring Torque and Drag Model

For the most simple torque and drag model the drillstring will be divided into several small segments. At the top and the bottom of each drillstring segment there is a node point. A measured depth and an inclination value is assigned to each of these node points. It is assumed that each of these drillstring segments is straight without any bending, therefore no bending moments occur in these models. The only forces acting are the gravitational forces due to the weight of the drillstring and the frictional forces.

The inclination of each small drillstring segment can be calculated using the inclinations from the bordering node points.

$$\bar{\theta} = \frac{\theta_i + \theta_{i+1}}{2} \qquad \text{Eq. 23}$$

$\bar{\theta}$…….. Average inclination of the segment
θ_i……..… Inclination of the wellbore in node point i [°]
θ_{i+1}…… Inclination of the wellbore in node point i+1 [°]

Using this average inclination of a drillstring segment, the tension or compression in each node point can be calculated by summing up the axial portion of the buoyed weight of each drillstring segment. Starting with the input data for the boundary conditions at the lowest node point, which is located on the lower end of the drillstring, the calculation procedure is done for every next higher node point. The boundary conditions for the lowest node point could be

either no tension at all (if the drillstring is hanging freely) or the weight-on-bit, if the drillstring is on bottom. After calculating the tensional force for every single node point, the tension in the uppermost node point should have the same value as the hookload measured on surface.

The tension in each node point can be calculated using the following equation, assuming that the drillstring is not moving:

$$F_{tension,i+1} = F_{tension,i} + w \cdot g \cdot \cos\bar{\theta} \qquad \text{Eq. 24}$$

Assuming that the friction factors are known for the wellbore, this simple torque and drag model can be adjusted to a moving drillstring by adding or subtracting the contribution of the frictional force. The frictional force of each drillstring segment can be calculated by multiplying the normal force of each segment with the friction factor valid for that segment:

$$F_{friction,i} = \mu \cdot F_N = \mu \cdot w \cdot g \cdot \sin\bar{\theta} \qquad \text{Eq. 25}$$

The tension in node point i+1 of a moving drillstring can then be obtained with the following equation:

$$F_{tension,i+1} = F_{tension,i} + w \cdot g \cdot \cos\bar{\theta} \pm F_{frition,i} \qquad \text{Eq. 26}$$

$F_{tension,i}$……Tension in node point i [N]
$F_{tension,i+1}$……Tension in node point i+1 [N]
$F_{friction,i}$…… Frictional force in node point i [N]
F_N……... Normal Force [N]
w……Buoyed weight of the drillstring segment [kg]
μ…….. Friction factor [ ]
g…….. Gravitational acceleration = 9.81 [m/s^2]

In case of a drillstring which is pulled out of the hole, the frictional force has to be added to the tension caused by the weight of the drillstring, resulting in a higher tensional load than for the drillstring in rest. If the drillstring is lowered into the borehole the contribution of the frictional force has to be subtracted, leading to a lower tensional load. The lowest parts of the drillstring

in a non-vertical well may even be under compression due to the friction when running the drillstring into the hole.

Advantages of the Softstring Torque and Drag Model

The simple torque and drag model described above has some obvious advantages. It is very simple and it is not very demanding concerning the performance of the computer. There are only a few input parameters. The inclination of each drillstring segment can be obtained from well survey data. The friction factor is a little bit more difficult to determine. It could be either estimated for each part of the hole, or it could also be calculated using the same torque and drag model. How this can be done will be described later in the work. Furthermore some drillstring data have to be entered. For the drag calculation it is sufficient to enter the weight per foot for the different drillstring sections. If the torque in the drillstring also has to be calculated, it is also necessary to enter the outer diameter of the tool joints connecting the different pieces of drillpipe.

Another advantage of that torque and drag model is that it could be extended rather easily. If the outer and inner diameters of the different parts of the drillstring are known, the cross-sectional area of the drillstring can be calculated. Knowing the tension in a certain node point and the cross-sectional area of the drillstring in that point, the axial stress in that node point can be determined, enabling stress analysis for the whole drillstring.

Another possible functionality that is easy to add to this model is the determination of the critical buckling loads. The dimensions of the casing and the open hole are needed as additional input parameters, as well as the material properties of the drillstring sections. Using these input parameters together with the ones from the original model, it is possible to calculate the critical buckling loads for sinusoidal and helical buckling in single every node point.

Shortcomings of the Softstring Torque and Drag Model

The simplicity of the model described above leads to a certain inaccuracy. Since every drillstring segment is assumed to be straight, no bending moments occur in the drillstring. Furthermore, the drillstring dimensions do not change, regardless if the drillstring is in tension or in compression. Under tension the drillstring will show an increase in length, whereas a drillstring under compression will have a reduced length. The apparent length of the drillstring will be even less if buckling occurs.

Using a model which does not account for the dimensional changes of the drillstring, it is not possible to model the influences of the different drilling dysfunctions like stick slip. In order to model these, advanced torque and drag models are necessary.

Friction

General Statements

Friction is one physical phenomenon which is not completely understood until now. The frictional force is induced by the counteraction between the surface molecules of the two bodies which are in contact with each other. It acts against a resultant force which is trying to move the body. The frictional force is independent of the contact area, but it is only dependent on the normal force between the bodies and the material properties of the two bodies. Furthermore the surface conditions of the two bodies are of importance. A lubricant between the bodies will greatly reduce the friction.

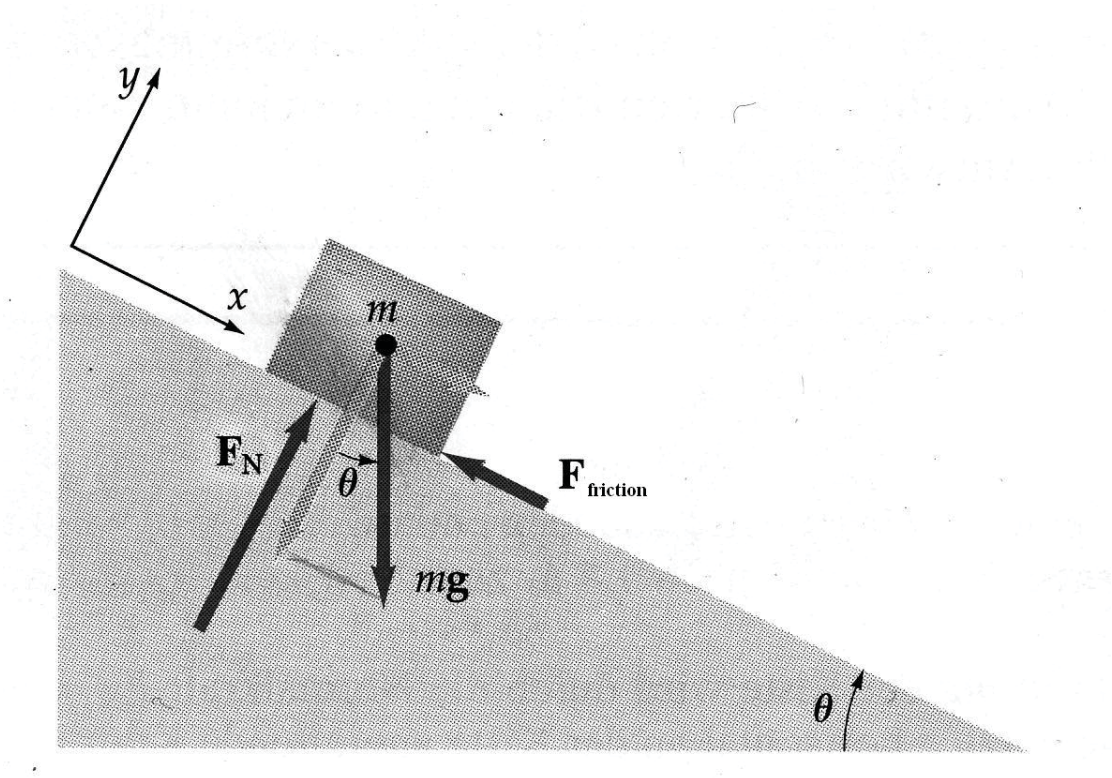

Figure 4 - Body on Inclined Surface

On the picture above one can see forces which are acting onto a body on an inclined surface. The frictional force acts against the tangential part of the gravitational force. As it can be seen in the equation below, the frictional force is only dependent on the normal fraction of the gravitational force and the friction factor μ. The friction factor is a dimensionless factor which incorporates the material properties, as well as the surface conditions.

$$F_{friction} = \mu \cdot F_N = \mu \cdot m \cdot g \cdot \cos\theta \qquad \text{Eq. 27}$$

$F_{friction}$…Frictional force [N]
F_N……. Normal force [N]
m…….. Mass [kg]
g…….. Gravitational acceleration = 9.81 [m/s^2]
α…….. Inclination [°]
μ…….. Friction factor [ ]

There are two different modes of friction: static friction and kinetic friction. As it can be seen on the picture below there is a linear relationship between resultant force applied to the body and static friction. The static friction has the same magnitude as the force applied to the body, but it acts in the different direction and prevents the body from moving. Once the force applied reaches a critical magnitude, the body starts to move. This critical force is equal to the maximum static frictional force. Once the force is bigger than this critical force, the body is in motion and the frictional force is in kinetic mode. In the kinetic mode, the frictional force, which resists the motion of the body, is independent of the force applied to the body, but only dependent of the normal force and the dynamic friction coefficient. Since the kinetic friction is lower than the static friction, it is simpler to keep a body in motion than to bring it in motion.

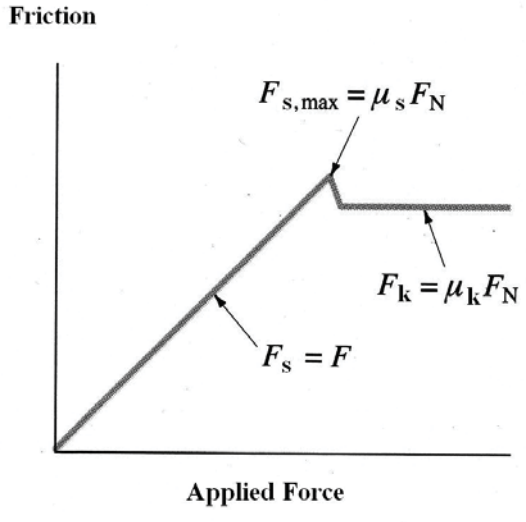

Figure 5 - Static and Kinetic Friction

When a body slides over a surface energy is transferred into heat and partly lost to the system. The energy converted to heat is given by the following equation:

$$E = \mu_k \int F_N \, dx \qquad \text{Eq. 28}$$

E……...Energy [J]
F_N……. Normal force [N]
μ_k……..Kinetic friction [ ]

Friction in Drilling Engineering

The fact that the static friction is much bigger than the dynamic friction is of great importance in drilling engineering. All torque and drag calculations require the friction factor between the drillstring and the borehole wall as input parameter. Drag of a non-rotating drillstring may limit the horizontal departure of an extended-reach well. Low friction trajectory profiles should remedy the problem of too high drag. But there are other issues concerned with friction. Axial force transfer during slack-off is influenced by friction, as not all of the energy is transferred through the drillstring to the bit, but may get lost due to friction. Some energy is transferred into thermal energy and is lost, other energy is saved in the drillstring because the drillstring acts like a spring. When the drillstring rotates again, the axial frictional force nearly equals zero and the energy saved in the drillstring is transferred down to the bit – this process usually occurs during stick-slip, and it may be very damaging to the bit.

Determination of Friction Factors in a Wellbore

The determination of the friction factors between the drillstring and the borehole wall is not simple. There are no logging methods which provide values for the friction factor. One common approach is to estimate the friction factor for the different sections of the well. For each section of the wellbore different friction factors will be assigned, based on experience from previous wells. A cased hole section has a lower friction coefficient than an open hole section, and the open hole section may have several different friction factors, depending on the geological formations to be drilled. Typical values for friction factors range from 0.1 to 0.4. Estimating friction factors usually lead to inaccurate results because the friction factor is not

only dependent on the formations drilled, but also dependent on the rheology of the mud, as well as the condition of the wellbore. Key seats, ledges and cavings in the borehole may greatly influence the friction in the wellbore. All of these contribute to the friction factor. The actual friction factor may therefore be completely different from the expected one.

By means of torque and drag calculations, two different friction factors can be calculated[2]: a wellbore friction factor and an incremental friction factor.

Pseudo Friction Factor

A wellbore friction factor is valid for the whole wellbore. It can be calculated using surface data input only. The calculation of the friction factor can be done for different operations, like picking-up, slacking-off and rotating off bottom.

The calculation of the wellbore friction factor has many benefits. It is very simple to calculate, not only regarding the calculation procedure, but also regarding the input data, because no real-time downhole data are needed for the calculation. Trendlines for friction factors can be determined when plotting the friction factor against the measured depth.

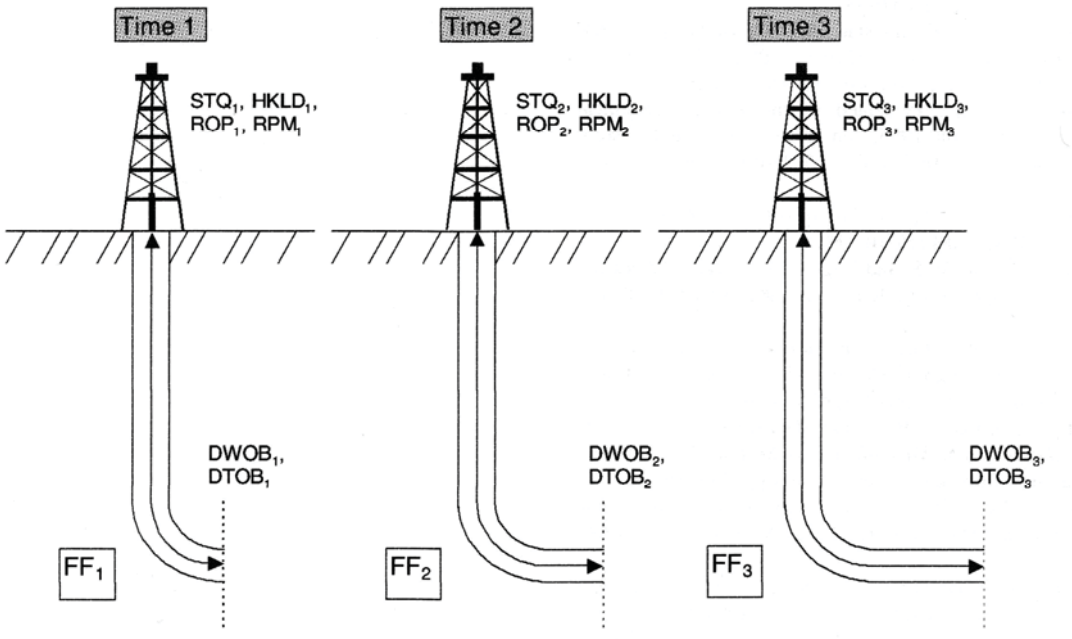

Figure 6 - Pseudo Friction Factor

On the other hand, the wellbore friction factor is not very useful for advanced torque and drag calculations. When using a mass-spring model for drillstring modelling, one will need a friction

factor for each segment of the wellbore. The behaviour of the spring-mass model will greatly depend on the friction factors of the different wellbore segments.

MATLAB Program for Calculation of a Pseudo Friction Factor

A MATLAB program shows the principle of the calculation. The input data consist of well survey data (measured depth, inclination and azimuth), drillstring data and drilling fluid data (mud weight). The user of the program also has to enter the hookload measured on surface while picking-up the drillstring. The program splits up the drillstring into a finite number of straight drillstring segments, each of them having an average wellbore inclination. Utilizing simple drag calculations, the program then uses different friction factors until the calculated hookload matches the real hookload measured on surface. Since the program calculates one single friction factor for the total wellbore, it does not differentiate between open hole and cased hole sections.

The following paragraphs describe the basic parts of that MATLAB application. The first part of the program generates equidistant survey data (measured depth, inclination and azimuth) from well survey data taken from different survey points.

After reading the data from the file, the user is prompted to enter the length of the drillstring, the weight per foot of the drillstring as well as the number of drillstring segments he wants to use for the calculation. At the beginning and the end of each drillstring segment there is one node point. Inclination and azimuth have to be calculated for all of these node points.

Using these inputs the program calculates values for inclination for each node point by means of a linear interpolation. Linear interpolation can be used for this process because it is assumed that the inclination angle increases or decreases linearly between two survey points, as stated by the minimum curvature calculation method.

Prior to the main part of the program, the calculation of the wellbore friction factor, the user has to input the hookload measured on surface. It is good practice to use the hookload data during tripping operations. The paper of Cardoso et al. [3] describes how to use the hookload as input data. This paper describes different patterns of hookload during tripping operations. On the picture one can see the hookload pattern for normal tripping operations, without any problems occurring.

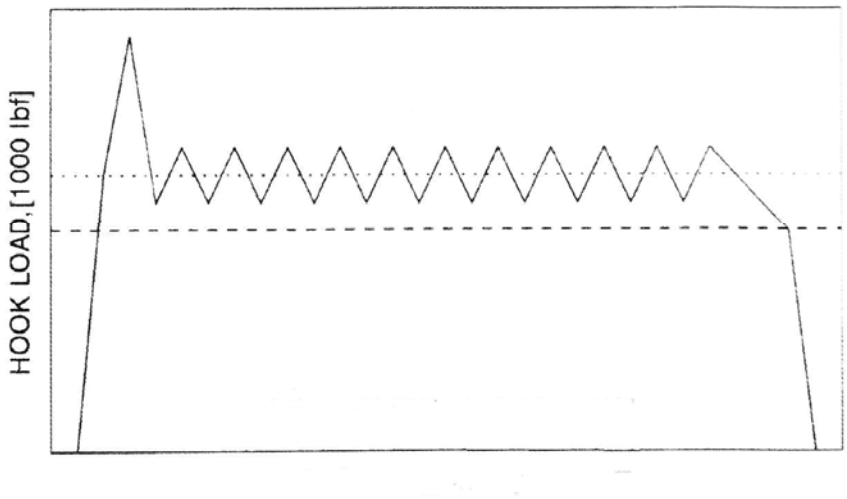

Figure 7 - Tripping Hookload Pattern

As it can be seen, the hookload value oscillates around an average value, which can be used as input value for the calculations. At the beginning and the end of each hoisting operation, the acceleration and deceleration effects dominate, so these values are not that useful as input data for the calculation of the friction factor. The hookload value of the middle portion of the graph is quite independent of the sampling rate used, so it can be even used with the 0.1 Hz data from the dataset which was used for this thesis.

The calculation of the wellbore friction factor is based on simple axial drag calculations. Every segment of pipe is assumed to be straight. Build-up and drop-off sections of the wellbore are no treated differently. Furthermore, no side bends are taken into consideration, so the program only uses the inclination values from the well survey data. It is also assumed that the mud weight in the pipe is the same as the mud weight in the annulus, so that the calculation could be achieved with using a simple buoyancy factor. Without the assumption of the same mud weights in and out of the pipe, the user would have to enter the different geometries of the drillpipe, as well as the stand-pipe pressure. The program would then have to calculate the weight of each drillpipe segment using advanced fluid dynamics calculations.

As mentioned before, the calculation of the wellbore friction factor could be done using hookload values when picking-up or slacking-off. In order to use this program, the user should enter the hookload value while picking-up the drillpipe during tripping operations. Nevertheless, the program can also be adjusted to slacking-off operations by just changing one sign in the calculation, as described in the next section. The advantage of calculating the friction factor during picking-up or slacking-off the drillpipe is, that no downhole parameters, such as weight-on-bit, are needed for the calculation.

The drag calculation starts at the very bottom of the pipe. Calculations of the axial tension in the pipe are made for every single node point. The tension of the pipe in each node point can be calculated using the following equation[4].

$$F_{i+1} = F_i + w \cdot g \cdot \cos\bar{\theta} + \mu \cdot F_N \qquad \text{Eq. 29}$$

F_N is the normal force between the drillpipe and the wellbore wall for one segment of drillpipe and can be calculated as follows:

$$F_N = w \cdot g \cdot \sin\bar{\theta} \qquad \text{Eq. 30}$$

The tension in the lowest node point is zero. Starting with this node point, the tension of each node point is then calculated using the equations above. In the end, the tension in the uppermost node point should match the hookload measured at surface. The only unknown parameter of the equation is the friction factor. This one is inserted into the equation by the program using a for-loop. The program inserts friction factors, starting with 0.01 for the first trial, with increments of 0.01 if the hookload calculated does no match the measured one. Once the hookload calculated is equal or greater than the hookload measured on surface, the program terminates and computes the friction factor that led to this result. This calculated factor is called wellbore friction factor, because the calculation makes no difference between the different sections of the wellbore.

The tension in each point of the drillstring is plotted at the end. At the very top of the drillsting the calculated tension then matches the hookload measured at surface, whereas at the bottom of the drillstring the tension is zero.

The program can easily be adapted to slacking-off action by changing the plus sign in the code of the weight calculation of each drillstring segment into a minus sign. The hookload has to be entered in the same manner. The hookload should be taken again from the middle part of the hookload tripping pattern, where the hookload is free of any acceleration and deceleration effects.

Incremental Friction Factor

Starting from a certain point of the wellbore, the incremental friction factor is then calculated in incremental steps. The big difference to the calculation of the wellbore friction factor is that the friction factor for a certain wellbore segment has to be stored. Each depth has then its corresponding friction factor, hence enabling more complex torque and drag calculations. Mass-spring models can also be set up when having incremental friction factors as input for the calculations.

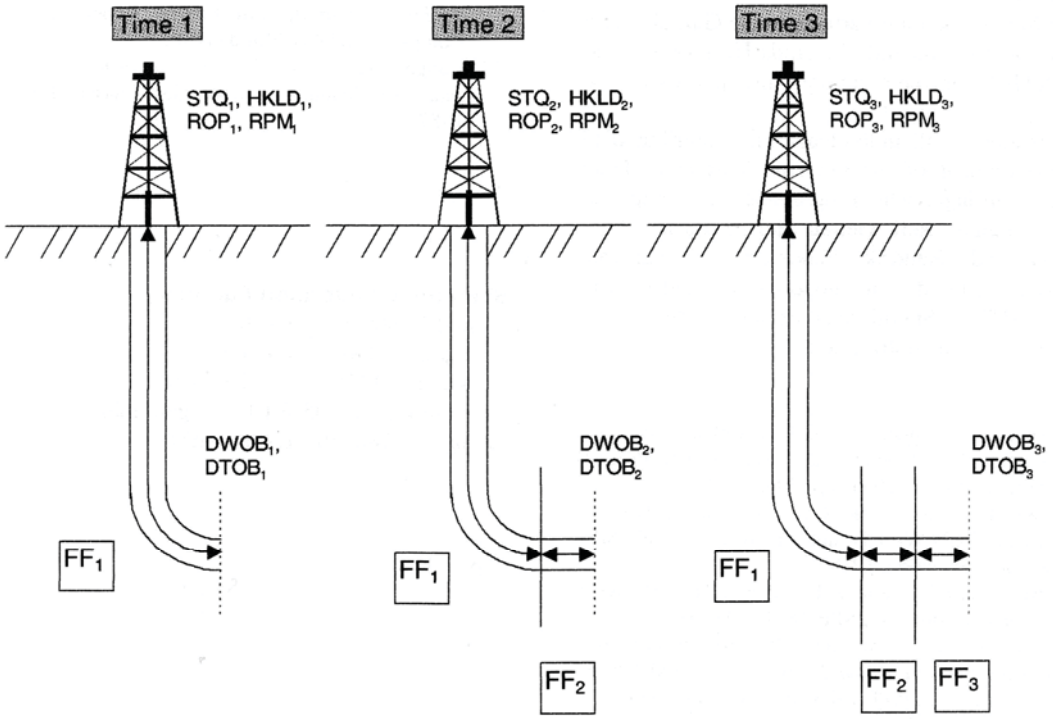

Figure 8 - Incremental Friction Factor

Data Organization

Challenges when Analysing Real-Time Data

Analysing real-time data is not a trivial task. Real-time data acquisition may lead to huge amounts of hard disk space needed, especially when data are sent in high frequency. Beside these problems there are also other problems to be solved. Real-time analysis of data requires high-performance computers because of the number of operations to be performed by the computer. Data provided by two or more different measurement providers may have differences in timestamps, although the data might have been recorded at the same time. Furthermore problems with data organization might arise. In order to have easy access to the data, all the data should be stored in databases rather than in different files. All these issues are of great importance for the process of data analysis.

Hardware Requirements

Analysing real-time data needs appropriate computer hardware. Very much hard-disk space is needed for real-time data acquisition. Even storing 1 Hz surfaced data from a mudlogging company for the total drilling duration of a well will lead to databases which occupy several gigabytes of hard-disk space. Since downhole data are recorded in much higher frequencies most of the times they will require even more hard disk-space. One should keep in mind that there might arise some problems during the drilling process of a well so that the drilling duration might be quite longer than actually planned. Therefore there should always be enough spare space on the hard-disks of a computer which is storing real-time acquisition data.

This issue is also of importance if the analysis process is not done in real-time, but, as for this thesis, after a well has been drilled. Since the well is already finished then, it is easy to determine how much hard-disk space will be required to save the data, making it easier to use an appropriate computer for the analysis of the data.

When storing the data in a database much disk-space could be saved using the right data types. In order to save the timestamps for 1 Hz surface data it is sufficient to store the values as *integer* instead of *double*. Doing so, not only the hard-disk space which is needed is reduced, but also the computer performance could be improved because every query can be performed faster. This can be done for all the channels where no values with floating points can be expected (i.e. total stokes of a pump).

The sizes of the different types of data in a MySQL database are shown in the following table:

Types	Data Type	Size in Bit
Integer Types	short	16
	int	32
	long	64
Floating Types	float	32
	double	64

Table 2

As it can be seen from the table, using *int* instead of *double* in a certain database will reduce the hard-disk space needed for the database entries by 50%. It is recommended to use the data type with the smallest size, but the data type should nevertheless be able to store all values which might be sent. It makes no sense to use *short* as data type, when the values which have to be stored in the database may be out of the range of the *short* data type.

Computer Performance

Real-time data acquisition is quite demanding concerning the performance of computers. Several tasks are running at the same time. There are applications which acquire the data, applications which write the data to a database and there might also be some applications which process the data in real-time. In order to analyse or process the data in real-time, many operations (i.e. filter or statistical operations to remove outliers from the data stream) are running at the same time. These operations might consume many of the computer's resources and may slow down the computer. In order to avoid problems with computer performance the processing services which need the most resources should run on different machines.

The next step to enable complex analysis processes without slowing down the performance of the processing computers too much would be the use of neural networks.

Different Timestamps

When analysing data from different data providers, for example from the mudlogger and from the directional driller, there may be a difference in the timestamps being sent. Therefore it might be quite difficult to compare data, because events actually happening at the same time might have different timestamps. One way to solve these problems is to use the system time of the data acquisition computer instead of the timestamps sent in the WITS records of the

data providers. Data streams of different providers will be saved with the computer's system-time timestamp in the database. By doing so it can be assured that data streams recorded at the same time by different providers have the same timestamp. Afterwards it is possible to compare the data from the different providers.

Nevertheless, this procedure might not be a solution for high frequency downhole data. Since it is not possible to pulse all of the data acquired by downhole measurement tools through the mud to the surface, the data have to be stored in a downhole memory. When the tool is brought to the surface again, the data stored in the downhole memory will be transmitted to a computer and stored in a database. From the data which were transmitted through the mud to the surface one can determine the offset between the timestamp sent with the WITS records from the downhole tool, and the timestamp of the data acquisition computer. This offset has to be taken into account prior to transferring the data from the downhole memory into the database. With this procedure it is assured that data for a specific event recorded by the mudlogging company and from the directional driller have the same timestamps.

Problems might arise when data sets from different providers are provided, but not in real-time but after a well has been completed. Then the procedure described above is useless because it is not possible to determine the difference in the computers' system times of the different providers. It has to be assured, nevertheless, that the data of the different providers could be compared, so the different data sets have to be correlated. One data set is the reference set. The timestamps of that set remain unchanged. All the events recorded by the different channels of the other data sets have to be correlated to the reference set afterwards. The timestamps of the other data sets have to be changed then to make sure that same events actually happen at the same time.

Universal Time Coordinated (UTC)

Universal Time Coordinated, abbreviated UTC, is a high-precision atomic time standard. It is counted in seconds, starting at January 1, 1970. The slowing of the earth is compensated by introducing leap seconds at irregular times. The geographical reference for UTC is the 0-meridian. Other timezones are expressed as positive or negative offsets from UTC. The Central European Timezone (CET), for example, would be expressed as UTC+1, which means that one hour (3,600 seconds) has to be added to the UTC timestamp in order to get the actual time in this timezone. Nevertheless, UTC should not be mixed up with Greenwich Mean Time (GMT), because GMT is only approximately the same with UTCs very precise atomic time scale.

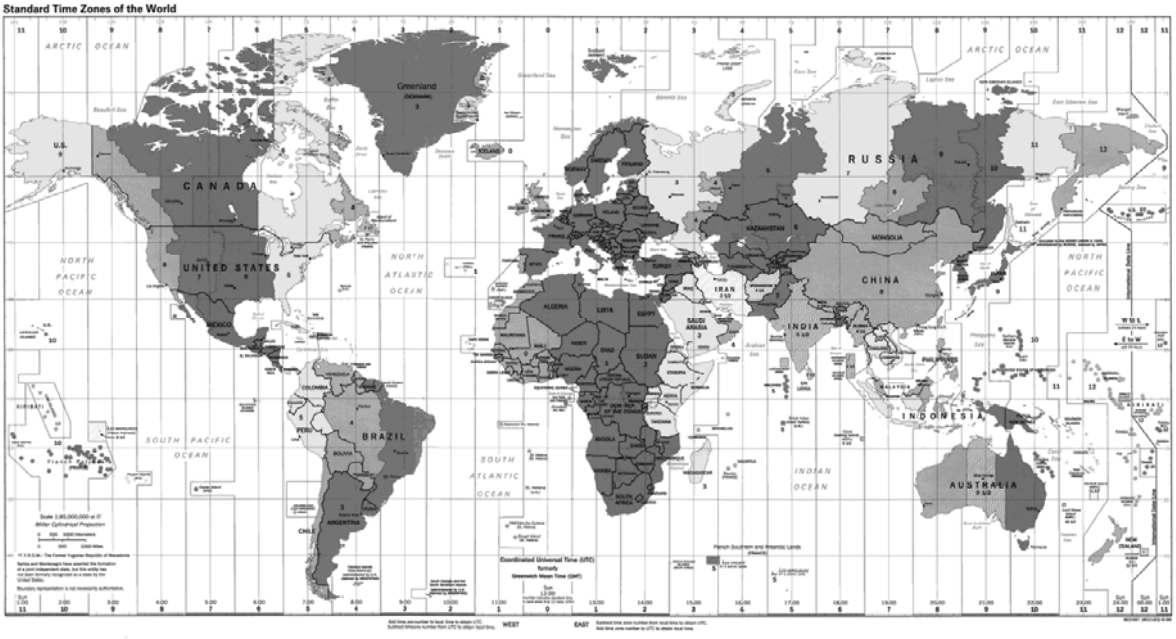

Figure 9 - UTC Offsets

The big advantage of UTC is that it is a high precise reference time, valid on the whole earth. Most of international multinational businesses, such as the aviation business, but also the oil industry, use UTC as their reference time. In aviation, for example, timetables (departure and arrival times of flights) are expressed in UTC.

The oil industry also makes use of UTC. In order to organize databases, reports from different parts of the world are not stored using the local times, but using UTC timestamps. As mentioned before, the local times then can be regained using the offsets to UTC.

The datasets for this thesis also have been converted to UTC before importing them to the MySQL database. The LAS-file with the data from the mudlogging company has a column with some sort of timestamp, but it was not a UTC timestamp, but had a different reference. For that reason this timestamp was useless for storing the data. The Microsoft Excel file which was provided in addition to the LAS-file had the same data as the LAS-file, but also a column with time entries. This time entries were then converted to UTC using the online converter from the internet page www.onlineconversion.com. Since there was no data provided regarding the location of the drilling site the time entries from the Excel-file were directly converted into UTC, without using any offset for a different timezone. The same procedure had to be done for the downhole data set. An additional pdf-file gave information about the start time of the downhole recording. This time was converted to UTC, again without using an offset. A MATLAB application then added the offset of each data record to that start timestamp in order to get the correct timestamps for each data record.

Databases

In order to organize the data effectively the data have to stored in a database rather than organizing the data in files. If the data would be saved in files it would be very difficult to analyse data afterwards, because it is very difficult to find the data which are needed for a certain analysis in all the files. Therefore it is common practice to store the data in a database. Many database software programs are in use, some of them are available for free, while others are commercial software packages. Microsoft Access is very famous, because it is available in the Microsoft Office package. Oracle is an example for another commercial database software. MySQL, which can be downloaded for free for non-commercial purposes from the internet, is a commonly used database program. The program is sufficient for most small and middle sized database projects. Furthermore it is simple to use, and there are many tutorials available on how to use this software.

Data Sets for the Thesis

The data provided for the thesis consisted of two datasets, one recorded on surface by a mudlogging company, and the other one recorded downhole using a special tool, called Isub-Tool.

Surface Data

The surface data set was delivered in a single LAS-file. Additionally, a Microsoft Excel file which contains the same data as the LAS-file was provided. The sampling frequency of the data was 0.1 Hz, so every 10 seconds there is one data record. The 12 channels which were recorded are:

- Measured depth of the hole
- Measured depth of the bit
- TVD of the hole
- Instant ROP
- Block position
- Hookload
- Standpipe pressure
- Surface torque
- Flowrate

- Downhole RPM
- Surface weight-on-bit
- Timestamp

The timestamp, which can be found in the LAS-file, is no UTC timestamp, but it has a different reference time. The UTC timestamp for every data record could be determined using the Excel-file, because the first column of the Excel-file shows the time when each data entry was recorded. This time has to be converted into a UTC timestamp for each record prior to storing the data in a database.
Each column in the LAS-file corresponds to one channel. The columns are tab-separated, so it is very easy to load the data into MATLAB using the *dlmread* function.

Using this function, all columns and rows are extracted loaded into MATLAB, where they can be split up into the different channels. It is useful to store all of the channels into a database in order to get easier access to the data. It is much easier to browse through all the data using database queries than doing this by hand.

Downhole Data

The high-frequency downhole data set was recorded using a downhole measurement tool.

Description of the Downhole Measurement Tool

The Isub-Tool[5] is a short downhole tool which is capable of recording several parameters with a very high sampling frequency (up to 250 Hz). The tool is equipped with accelerometers, strain gauges and one magnetometer. Using these sensors the tool is capable of measuring the axial, lateral and angular accelerations, the angular position and the forces and moments acting on the tool. Since the data are recorded in a very high frequency, the tool also has a downhole memory to store the data. The tool is easy to use and does not need any special crew to set up and start. The start of the data recording is triggered automatically when the tool is made up on the drillstring.

Description of the Data

The downhole data set for the thesis was provided in several dat-files. These files were simple tab-delimited ASCII-files. The different channels were organized in columns, with each row in the file being equal to one data record.

The channels which were recorded by the tool are:

- Lateral acceleration in positive X-direction
- Lateral acceleration in negative X-direction
- Lateral acceleration in positive Y-direction
- Lateral acceleration in negative Y-direction
- Tangential acceleration
- Axial acceleration
- Axial force
- Torque
- Bending moment
- Angular Position

No timestamp was delivered with the files. The start time of the data recording could be determined using the pdf-file which contained additional information. The sampling frequency of the data recording was 50 Hz, so every 20 milliseconds there is a data entry. Each file has 360,000 rows, therefore each file is covering two hours of data recording. Nevertheless it was not that easy assigning the timestamps to the data records, because there was the information in the pdf-file that the data recording stopped every 10 minutes for 2.56 seconds. So every dat-file containing the recorded data was covering two hours of recording time, but two hours and 30.72 seconds actual time. These recording stops have to be taken into account before importing the data into the database.

The start time provided in the pdf-file was converted into a UTC-timestamp using the online conversion from the internet page www.onlineconversion.com. Starting with this UTC-timestamp a MATLAB application then assigned the correct UTC-timestamp to every data entry, also taking the gaps caused by the recording stops into account.

Prior to importing the downhole data set into the database it had to be checked whether the downhole data could be correlated to the surface data or not. Unfortunately this was not the case. Therefore the downhole data set had to be shifted back by a little bit more than 300 seconds in order to have the same events happen at the same time. The timestamps of the surface data set were used as reference timestamps in this case.

Issues with Raw Data

Several issues are concerned with handling the raw data, especially the high frequency data recorded downhole. One has to be aware, that the data recorded with the downhole tool are not recorded directly at the bit, but in a certain distance away from the bit. All the values for the

different channels have to be corrected in order to get the values which correspond to the bit itself.

Correction of the Axial Force

The axial force recorded with the downhole tool is not equal to the weight-on-bit, because of the distance between the bit and the tool. The pressure exerted by the drilling fluid as well as the weight of the bottom-hole assembly below the tool have to be taken into account, when correcting the values recorded by the downhole tool. In order to correct the values, some additional information is needed.

To enable a pressure correction, the vertical hole of the well at the point of interest is needed, as well as the weight of the drilling fluid. With these values the hydrostatic pressure at the depth of interest can be calculated. The difference between hydrostatic pressure and dynamic pressure will be neglected here, since no values for the pressure losses at the bit and the annular pressure losses are given.

In order to make a correction of the axial force for the weight of the bottom-hole assembly below the downhole measurement tool, the weight of the bottom-hole assembly has to be determined. The tension in the tool just prior to disconnecting it from the drillstring gives the buoyed weight of the bottom-hole assembly. The true weight can be determined from this value if the mud weight is also known.

Supposed that the area of the tool is known, the force exerted by the fluid pressure in a certain depth can be calculated. This force is then used to correct the tension measured by the downhole tool. The weight of the bottom-hole assembly is also used for correction purposes. Without these corrections it would be impossible to determine the weight-on-bit by using the measurements of the downhole tool.

Frequency Aspects

The measured parameters from the two data providers have different sampling frequencies. Due to this difference it is nearly impossible to correlate the data, because there are 500 data points recorded downhole, whereas in the same time there is only one data point recorded on surface. Analysis is therefore limited to detection of different events happening downhole by means of surface measurements.

Drilling Dysfunctions

Drilling dysfunctions influence the drilling process in an undesired manner, each of them may be harmful in its specific way. Buckling influences the axial force transfer through the drillstring to the bit, and it may also damage the drillpipe and its tool joints. Stick-slip is another drilling dysfunction which is very likely to occur when drilling with PDC bits. This dysfunction may be damaging to the bit, because the energy stored in the drillstring during the sticking phase will suddenly be released and transferred down to the bit during the slipping phase. Bit bounce is a drilling dysfunction that is related to drilling with roller cone bits. High axial accelerations and forces acting on the bit are the characteristic signs of this drilling dysfunction.

Many papers have been published about the different drilling dysfunctions. The most important aspects of them will be summarized on the next pages, as well as some proposals about how to detect these drilling dysfunctions using surface measurements.

Drillpipe Buckling

Buckling of the drillpipe is probably the most well known drilling dysfunction, although it is also only described by empirical equations. Drillpipe buckling is the deformation of the drillstring under compression. Therefore buckling can only occur in the sections of the drillstring which are compressed. Most of the time, these are the lowest sections of the drillstring. However, when drilling a horizontal well for example, the section just above the build section may be under compression, too. If the compressive load on the drillstring gets too high, the drillstring will start to buckle. If the compressive force in a drillpipe reaches a certain threshold value, the drillpipe will start to buckle. There are two different modes of buckling which are generally accepted in the literature:

- Sinusoidal buckling
- Helical buckling

According to the paper of Kuru et al. [6] there is also an intermediate form of buckling between the sinusoidal buckling and the helical buckling, the so called unstable sinusoidal buckling. Nevertheless, the industry generally uses only two modes of buckling.

Factors influencing Buckling

There are several factors which influence the occurrence of buckling. The main factor is the force of compression. The higher the compressive force, the more likely the drillpipe will tend to buckle.

The stiffness of the drillpipe also has a great influence on the buckling resistance. The higher the stiffness of the pipe, the less likely buckling of the drillpipe will occur. The stiffness of a specimen not only depends on its material, but also on the dimensions of the specimen. The axial stiffness of a certain body can be calculated using the following equation:

$$k = \frac{A}{l} \cdot E \qquad \text{Eq. 31}$$

k……Axial stiffness [N/m]
A……...Area [m^2]
l…….Length [m]
E…….. Modulus of elasticity / Young's modulus [N/m^2]

As it can be seen, the higher the ratio of the cross-sectional area to the length of the body, the higher is the stiffness. Furthermore, materials with a higher Young's modulus also have higher stiffness. Drill collars have higher stiffness than drillpipes, because the cross-sectional area of the drill collars is higher than that of drillpipes. Therefore drill collars are less susceptible to buckling and should be used in the regions where the drillstring is under compression.

Another factor influencing the occurrence of buckling is the clearance between the drillpipe wall and the wall of the casing or the open hole. The less space between the two walls, the less likely buckling will set in.

The drilling fluid which is pumped down through the drillpipe also might have an influence on buckling. Normally, a fluid which is pumped under high pressure through a pipe or a hose tends to straighten its conductor. This statement is not true for drilling operations. As stated in the paper of Kuru et al. [6] the effect of internal fluid pressure on the buckling behaviour is negligible.

Buckling Modes

There are two different buckling modes which are generally accepted by the drilling industry, the sinusoidal buckling and the helical buckling.

Sinusoidal Buckling

The critical compressive force at which the drillpipe will start to buckle sinusoidally can be calculated by the following equation (in field units). Note that this equation is valid for inclined and horizontal wells:

$$F_{crit,s} = 2\sqrt{\frac{E \cdot I \cdot w \cdot \sin\alpha}{r}} \qquad \text{Eq. 32}$$

The area moment of inertia, denoted with I in the equation above, is calculated by the following equation:

$$I = \frac{\pi}{64}\left(OD^4 - ID^4\right) \qquad \text{Eq. 33}$$

The equation above is only valid for inclined wellbores. In the case of a vertical wellbore the equation (in field units) is different:

$$F_{crit,s} = 1.94\sqrt[3]{EI \cdot w^2} \qquad \text{Eq. 34}$$

$F_{crit,s}$…. Critical sinusoidal buckling load [lbf]
E…….. Modulus of elasticity / Young's modulus [psi]
I……. Area moment of inertia [in^4]
w…….. Buoyed weight of the drillstring [lbm/ft]
r……. Radial clearance between the drillpipe and the borehole wall [in]
OD……Outer diameter of the drillpipe [in]
ID……. Inner diameter of the drillpipe [in]
α…….. Inclination of the wellbore [°]

Helical Buckling

The critical force for helical buckling is usually expressed by multiplying the critical force for sinusoidal buckling by a certain factor. Several factors have been suggested by different authors. The factors range from 1.41 to 1.83 [7]. The paper of Kuru et al. [6] suggests using the following equation to calculate the critical buckling load in inclined wellbores (in field units):

$$F_{crit,h} = 2\sqrt{2} \cdot F_{crit,s} \qquad \text{Eq. 35}$$

The multiplication factor again is different in the case of a vertical wellbore. The critical helical buckling load in a vertical wellbore can be calculated as follows (in field units):

$$F_{crit,h} = 5.55 \sqrt[3]{EI \cdot w^2} \qquad \text{Eq. 36}$$

$F_{crit,h}$…. Critical helical buckling load [lbf]
$F_{crit,s}$…. Critical sinusoidal buckling load [lbf]
E…….. Modulus of elasticity / Young's modulus [psi]
I…… Area moment of inertia [in^4]
w…….. Buoyed weight of the drillstring [lbm/ft]

Consequences of Buckling

Drillpipe buckling may lead to big problems during the drilling process. The problems caused by buckling range from drillpipe and tool joint failure to the sharp increase in friction which might lead to a stop of axial force transfer. The problem with the axial force transfer will be described in more detail later in the work, by describing the normal forces which increase the friction related with buckling.

When drilling a wellbore, it may be very difficult to avoid buckling in certain parts of the drillstring. This is not a big issue, as long as helical buckling can be avoided. Helical buckling should be avoided under any circumstances, because the sudden increase in friction will soon lead to a lock-up condition, where any further slack-off of weight will not lead to a weight transfer to the bit, but worsen the problem.

Contact Forces

Drillpipe buckling will induce additional contact forces between the drillpipe and the borehole wall. According to Coulomb's friction law, these contact forces will result in higher frictional resistance against and movement of the drillstring. If the friction gets too high, axial force will not be transferred through the drillstring any more, but only result in higher axial loads, which will make the problem even worse. This condition is called 'lock-up'.

The paper of Kuru et al. publishes a set of equations which can be used to calculate the contact forces of a buckled drillpipe.

The contact force for a helically buckled drillpipe in a vertical pipe is given by:

$$N = \frac{r F_{comp}^{\ 2}}{4 \cdot EI} \qquad \text{Eq. 37}$$

N…….. Unit normal force [lbf/ft]
r……. Radial clearance between borehole and pipe [in]
F_{comp}… Axial compression force [lbf]
E…….. Modulus of elasticity / Young's modulus [psi]
I……. Area moment of inertia [in^4]

The equations to calculate the contact forces of a straight pipe, a sinusoidally buckled pipe and a helically buckled pipe in an inclined wellbore are as follows:

$$N = w \sin \alpha \qquad \text{Eq. 38}$$

$$N = \frac{16\pi^4 EIrA^2}{p^4}\left(-A^2 \cos^4 \frac{2\pi z}{p} + 3\sin^2 \frac{2\pi z}{p} - 4\cos^2 \frac{2\pi z}{p}\right) + \frac{4\pi^2 rFA^2}{p^2}\cos^2 \frac{2\pi z}{p} + w \sin\alpha \cos\theta$$

Eq. 39

$$N = \frac{rF^2}{4EI} + w \sin\alpha \cos\theta$$ Eq. 40

N…….. Unit normal force [lbf/ft]
w…….. Buoyed unit weight of the pipe [lbf/ft]
α…….... Inclination of the borehole [°]
r……. Radial clearance between borehole and pipe [in]
F_{comp}… Axial compression force [lbf]
E…….. Modulus of elasticity / Young's modulus [psi]
I……. Area moment of inertia [in^4]
A…….. Amplitude of pipe sinusoidal configuration [rad]
p…….... Length of a sine curve / length of a pitch of a helix [ft]
z……Distance along the centreline of the inlined wellbore [ft]
θ…….... Angular displacement of pipe [rad]

For the wellbore sections of constant curvature, the following set of equations, again for the unbuckled pipe, for a pipe in sinusoidal buckling mode and for a helically buckled drillpipe, should be used:

$$N = \frac{F_{comp}}{R} + w \sin\alpha$$ Eq. 41

$$N = \frac{16\pi^4 EIrA^2}{p^4}\left(-A^2\cos^4\frac{2\pi z}{p} + 3\sin^2\frac{2\pi z}{p} - 4\cos^2\frac{2\pi z}{p}\right) + \frac{4\pi^2 rA^2}{p^2}\left(F_{comp} + \frac{EI}{R^2}\right)\cos 2\frac{2\pi s}{p} + \left(\frac{F_{comp}}{R} + w\sin\alpha\right)\cos\theta$$ Eq. 42

$$N = -\frac{16\pi^4 EIr}{p^4} + \frac{4\pi^2 r}{p^2}\left(F_{comp} + \frac{EI}{R^2}\right) + \left(\frac{F_{comp}}{R} + w\sin\alpha\right)\cos\theta$$ Eq. 43

N…….. Unit normal force [lbf/ft]

w…….. Buoyed unit weight of the pipe [lbf/ft]
α…….. Inclination of the borehole [°]
R…….. Radius of curvature of a borehole [ft]
r……. Radial clearance between borehole and pipe [in]
F_{comp}… Axial compression force [lbf]
E…….. Modulus of elasticity / Young's modulus [psi]
I……. Area moment of inertia [in^4]
A…….. Amplitude of pipe sinusoidal configuration [rad]
p…….. Length of a sine curve / length of a pitch of a helix [ft]
z……Distance along the centreline of the inlined wellbore [ft]
θ…….. Angular displacement of pipe [rad]

The amplitude of the sine curve, A, the angular displacement, θ, and the length of the sine curve, p, are needed for the calculation of the contact forces.

The relationship between axial compressive force and the amplitude of the sine curve is given by:

$$F_{comp} = 2\sqrt{\frac{EIw\sin\alpha\left(\frac{3}{2}A^2+1\right)\left(1-\frac{A^2}{8}\right)}{r}} \qquad \text{Eq. 44}$$

F_{comp}… Axial compression force [lbf]
w…….. Buoyed unit weight of the pipe [lbf/ft]
α…….. Inclination of the borehole [°]
E…….. Modulus of elasticity / Young's modulus [psi]
I……. Area moment of inertia [in^4]
A…….. Amplitude of pipe sinusoidal configuration [rad]

Knowing the amplitude of the sine curve, the angular displacement and the length of the sine curve can be calculated for a drillpipe in sinusoidal buckling mode:

$$\theta = A\sin\left(\frac{2\pi z}{p}\right) \qquad \text{Eq. 45}$$

θ…….. Angular displacement of pipe [rad]
A…….. Amplitude of pipe sinusoidal configuration [rad]
p…….. Length of a sine curve / length of a pitch of a helix [ft]
z…… Distance along the centreline of the inlined wellbore [ft]

$$p = 2\pi \sqrt{\frac{EIr\left(\frac{3}{2}A^2 + 1\right)}{w \sin\alpha\left(1 - \frac{A^2}{8}\right)}} \qquad \text{Eq. 46}$$

p…….. Length of a sine curve / length of a pitch of a helix [ft]
w…….. Buoyed unit weight of the pipe [lbf/ft]
α…….. Inclination of the borehole [°]
E……. Modulus of elasticity / Young's modulus [psi]
I…… Area moment of inertia [in^4]
A…….. Amplitude of pipe sinusoidal configuration [rad]
r…… Radial clearance between borehole and pipe [in]

For a sinusoidally buckled pipe in a curved wellbore the distance along the centreline of the inclined borehole, z, has to be replaced by the distance along the centreline of the curved borehole, s.
For a drillipipe in helical buckling mode the equations for the angular displacement and pitch of the helix look as follows:

$$\theta = \frac{2\pi z}{p} \qquad \text{Eq. 47}$$

$$p = \sqrt{\frac{8\pi^2 EI}{F_{comp}}} \qquad \text{Eq. 48}$$

θ…….. Angular displacement of pipe [rad]
z…… Distance along the centreline of the inlined wellbore [ft]
p…….. Length of a sine curve / length of a pitch of a helix [ft]

F_{comp}… Axial compression force [lbf]
E…….. Modulus of elasticity / Young's modulus [psi]
I……. Area moment of inertia [in^4]

Again, if the wellbore is curved instead of straight, the distance along the centreline of the inclined wellbore, z, has to be replaced by the distance along the centreline of the curved borehole, s.

Detection of Buckling

Buckling of the drillpipe can be detected using torque and drag models. Even when using simple torque and drag models, which do not account for the change in drillstring dimensions, it is possible to calculate the axial force in the drillstring in the node points, as well as the critical buckling loads for sinusoidal and helical buckling. The drilling engineer is then able to see area of potential drillpipe buckling and can take preventive action against it by changing the drilling parameters (for example less weight-on-bit) or by changing to drillipipe with more stiffness.

Stick-Slip

Stick-slip is a well known and well investigated type of self-induced torsional vibrations. It is characterized by a periodical sticking and slipping phase of the drillstring or the bit. During the sticking phase parts of the drillstring or the bit are at rest and not moving at all. After sufficient torque has been built up, the drillstring becomes free again and is moving with much higher rotational speeds than during normal drilling. Rotational speeds can reach hundrets of rpm during the first moments of the slipping phase. After being slowed down, the drillstring will stick again and the whole process starts again. The stick-slip process leads to torque and rotational speed oscillations along the entire drillstring. The oscillation period depends on several factors, like the length and the properties of the drillstring, the rotational speed at the top of the drillstring and also the nature of the friction. Usually the stick-slip frequency is below 1 Hz, with typical values ranging from 0.05 Hz to 0.5 Hz [8].

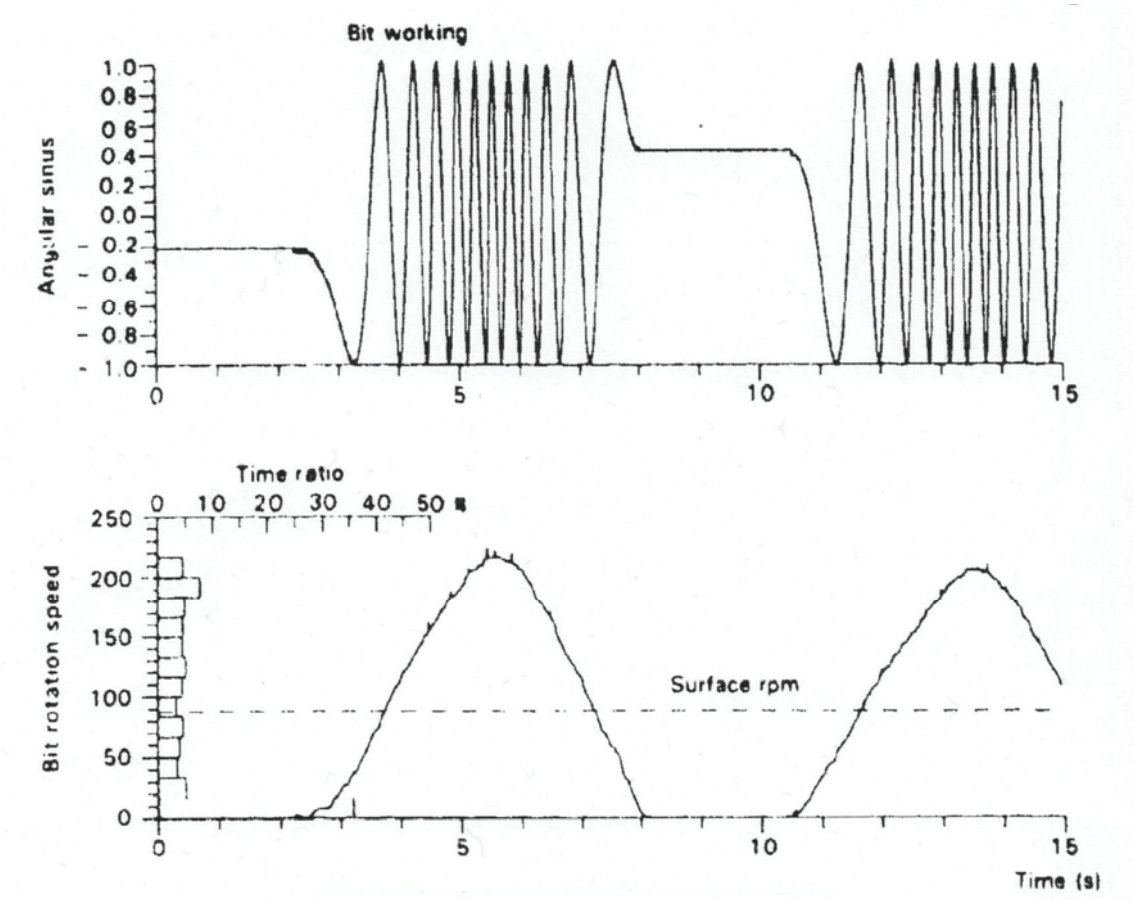

Figure 10 - Angular Position and RPM during Stick-Slip

Stick-slip is very harmful to the downhole equipment, especially the bit. During the sticking phase no axial force will be transferred to the bit due to the high friction. This axial force will be stored as potential energy in the drillstring, similar to the potential energy stored in a spring during compression. As soon as the drillstring starts rotating again during the slipping phase, the axial friction nearly equals zero and all the stored energy will be transferred as axial force down to the bit. This sudden force transfer may result in very high and harmful weight-on-bit. The shock loads not only damage the bit, but also other downhole equipment.

Factors influencing Stick-Slip

Several factors influence the occurrence of stick-slip. Among these factors are the operating conditions, especially the rotational speed and the weight-on-bit, the bit and other factors like the drilling fluid and the formations to be drilled.

Operating Conditions

The operating conditions have a big influence on the occurrence of stick-slip. The most important operating conditions to be controlled in order to avoid stick-slip are the rotational speed and the weight-on-bit. Several papers [9] present the results of numerous investigations about the influence of these factors on the occurrence of stick-slip vibrations.

The rotational speed of the drillstring plays an important role when trying to avoid stick-slip vibrations. Field tests have shown that there is a critical rotational speed above which stick-slip is not likely to occur. Below this critical speed torsional waves in the drillstring may be generated. These torsional waves may then induce stick-slip vibrations. Since many other parameters play together, it is not possible to forecast this critical rotational speed with sufficient accuracy.

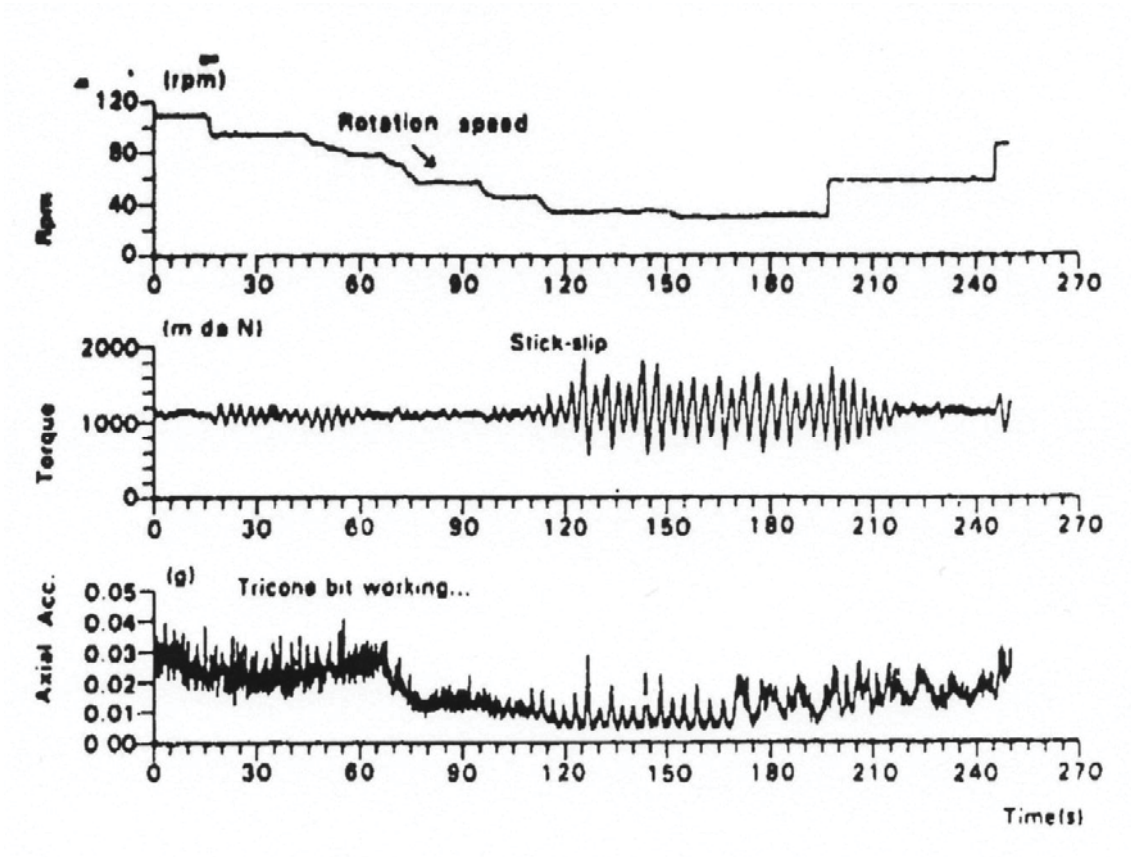

Figure 11 - Effect of Bit RPM on Stick-Slip

The effect of weight-on-bit on stick-slip is also well investigated. Generally, it can be stated that the higher the weight-on-bit, the more likely stick-slip vibrations will occur. Due to bending moments in the bottom-hole assembly resulting from higher weight-on-bit, the stabilizers or the drill collars will be pushed even more against the borehole wall. This might directly lead to stick-slip vibrations. On the other hand, lower weight-on-bit will result in more regular bit behaviour.

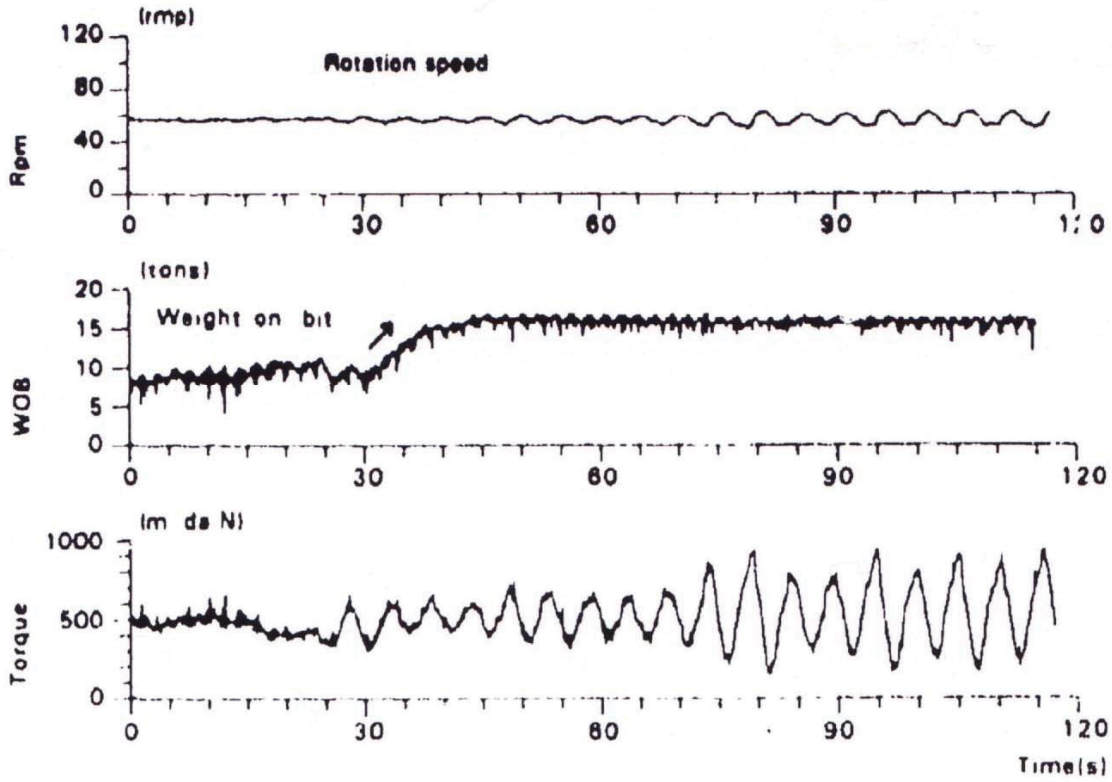

Figure 12 - Effect of Weight-on-Bit on Stick-Slip

The relationship between rotational speed and weight-on-bit has also been investigated. Higher rotational speeds are required to avoid stick-slip vibrations when using a high weight-on-bit. The lower the weight-on-bit, the lower the critical rotational speed above which stick-slip will not occur.

Bit

Although stick-slip vibrations may occur at any type of bit, they are more likely to set in when PDC bits are used. Roller cone bits are less prone to stick-slip. As described in the paper of Dufeyte et al. [9], during one drilling campaign in the Mediterranean Sea only the PDC bit showed stick-slip vibrations, while the roller cone bits did not. Since the other parameters like formations to be drilled, well profile, drillstring design and the operating conditions where comparable between the wells, the only reason for the stick-slip vibrations could be the nature of the bit itself.

The frequency of the stick-slip vibrations is not much dependent on the bit type, but on other parameters. In the paper of Chen et al. [10] it is pointed out that “once initiated, stick-slip

frequency is dependent on the bottomhole assembly (BHA) rather than bit type or bit-formation interaction". As an example the stick-slip frequency for a roller cone bit and a PDC bit in a certain wellbore was determined. Each bit had a stick-slip frequency of about 0.7 Hz, which was close to the first torsional natural frequency of the drillstring.

Drillstring

The type of drillpipe is one of the main factors influencing the development of stick-slip in the drillstring. When drilling a formation porne to stick-slip the stabilizers have the most influence on the occurrence of stick-slip as torsional waves develop when the stabilizer crosses a layered formation.

Lithology

The lithology of the formations to be drilled may be the factor which has most influence on the development of stick-slip. When drilling highly stratified formations stick-slip is very likely to occur, as torsional waves are developing when the near-bit stabilizers cross a clayey layer.

The paper of Pavone et al. [8] points out, that stick-slip is more likely to develop in harder rocks than in softer ones.

Well Profile

The well profile influences the development of stick-slip because of the influence on friction. It was reported that a vertical well created such favourable conditions for the occurrence of stick-slip because of its nature of friction between the drillstring and the borehole wall [9].

Other factors

The influence of the drilling fluid on the development of stick-slip is not well investigated.

Consequences of Stick-Slip

Due to the uncontrolled, sudden force transfer it is very difficult for the driller to keep the weight-on-bit between certain limits. During the slipping phase the drillstring will release its stored potential energy, which will be transferred down to the drillstring. This may cause very high values for weight-on-bit, which, as a consequence, will shorten the life of the bit. The high accelerations which occur during the process of energy release are not only damaging for the

bit, but also for any other type of downhole tool. Early fatigue of downhole equipment is one of the major consequences when drilling under stick-slip conditions.
On the other hand, the occurrence of stick-slip has no major influences on the rate of penetration. Drilling under stick-slip conditions will reduce the rate of penetration, but only for to a small extend. The paper of Pavone et al. [8] cites a publication where a 12% reduction in rate of penetration was observed, while the paper of Chen et al. [10] points out, that drilling under stick-slip conditions does not adversely affect the rate of penetration.

Detection of Stick-Slip

There are several ways proposed how to detect stick-slip using surface measurements only. Since the fluctuations of torque and rpm are transferred through the whole drillstring up to the surface, these can be used for stick-slip detection.

Several drilling runs of one well have been investigated for this thesis. The results obtained have been verified using the measurements taken by the downhole tool. Since this tool has a magnetometer which is used to record the angular position of the tool, it was able to check whether it is possible to set up a MATLAB program capable of detecting stick-slip using surface measurements only. Furthermore other aspects of stick-slip, like the lateral accelerations present during stick-slip or the behaviour of other surface parameters, have been investigated.

Many papers propose to use the torque measured at surface for stick-slip detection. An alternative way has been proposed by Desmette et al. [5]. As it is suggested in their paper, stick-slip can be detected by calculating a so called stick-slip index using the rotational speed measured at surface as input. This index is then used to determine how likely it is that the drilling process is conducted in a stick-slip regime.

The stick-slip index is calculated in a similar manner as the torque index proposed in the other papers. First the height of the envelope curve in a time-based view of the surface rpm has to be determined. By dividing the height of the envelope curve by a running average value for the surface rpm, the stick-slip index is obtained. An index of zero would indicate that there is no stick-slip occurring, whereas an index of one would tell the user that there is a pure stick-slip regime.

A MATLAB application has been set up in order to calculate the stick-slip index for the data. In order to achieve that, MATLAB was used together with MATLAB's Signal Processing Toolbox. The Signal Processing Toolbox is offering powerful tools when dealing with different signal data streams. The tools from the toolbox is can not only be used to plot signals and analyse their spectrums, but they can also be used for filtering issues, like filter design and analysis.

The tool which was used for calculation of the stick-slip index was the *SPTool*. This tool can be used for plotting signals, spectral analysis of these signals, as well as for filtering.

For calculation of the stick-slip index the spectral analysis and the filter design tools of the *SPTool* are not needed. Only the signal plotting tool is used. Per default there are different signals already loaded into the tool. In order to analyse the rpm signal it has to be imported into the tool. This can be done by choosing the import option from the *File* menu. After importing the signal, it can be plotted and viewed by clicking onto the *View* button at the lower end of the list field.

A new window, called *Signal Browser*, will open after clicking onto the *View* button. The main part of the window shows a graphical representation of the signal.

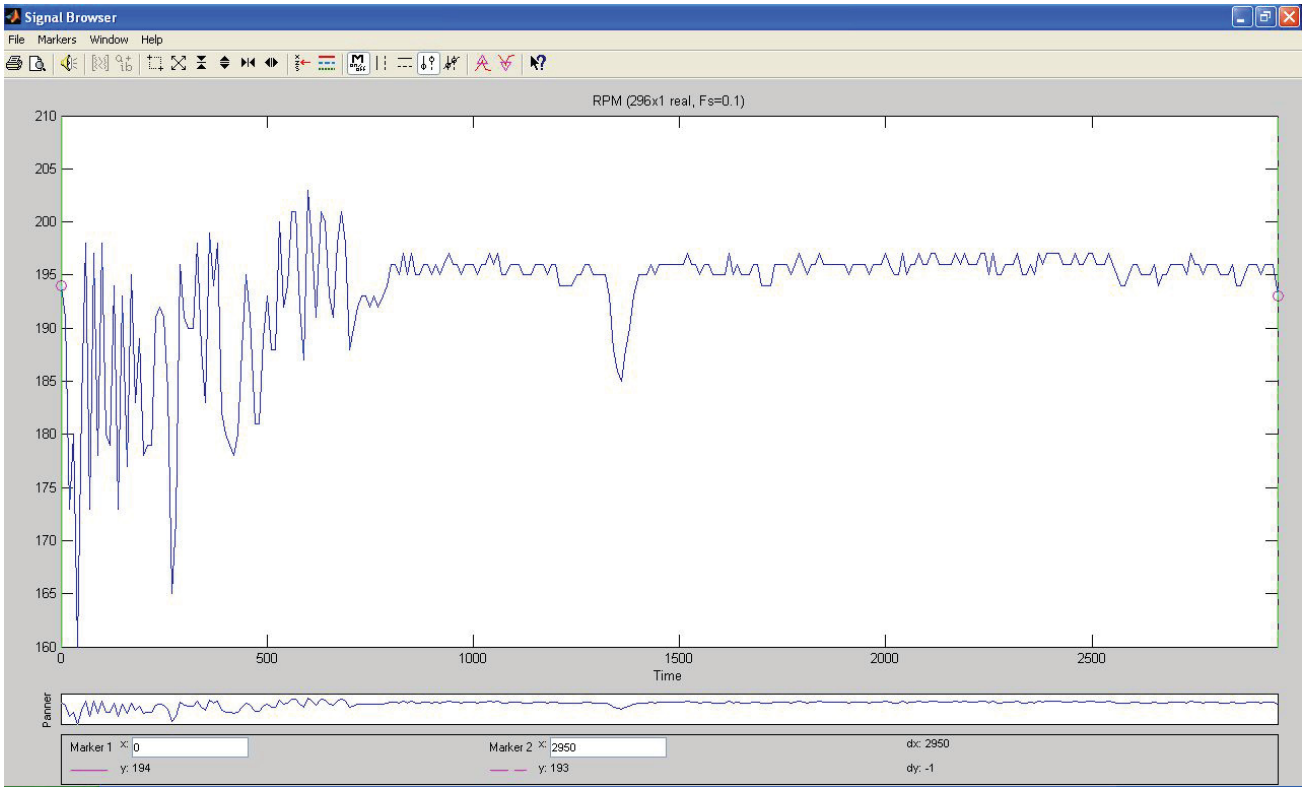

Figure 13 - Signal Browser

The functionality of the tool that is needed for the calculation of the stick-slip index is the possibility to set different markers. There are several markers that can be set, including horizontal markers and vertical ones. The markers that are used for the calculation process are the markers for peaks and valleys of the signal. By clicking onto *Peaks* and *Valleys* in the *Markers* menu, all the peaks and valleys for that signal will be marked by small, pink triangles. The peaks and valleys are used in the next calculation step in order to get the envelope curve.

In order to make use of the marked values they have to be exported again to the MATLAB workspace. This can be done by choosing the *Export* option from the *Markers* menu.

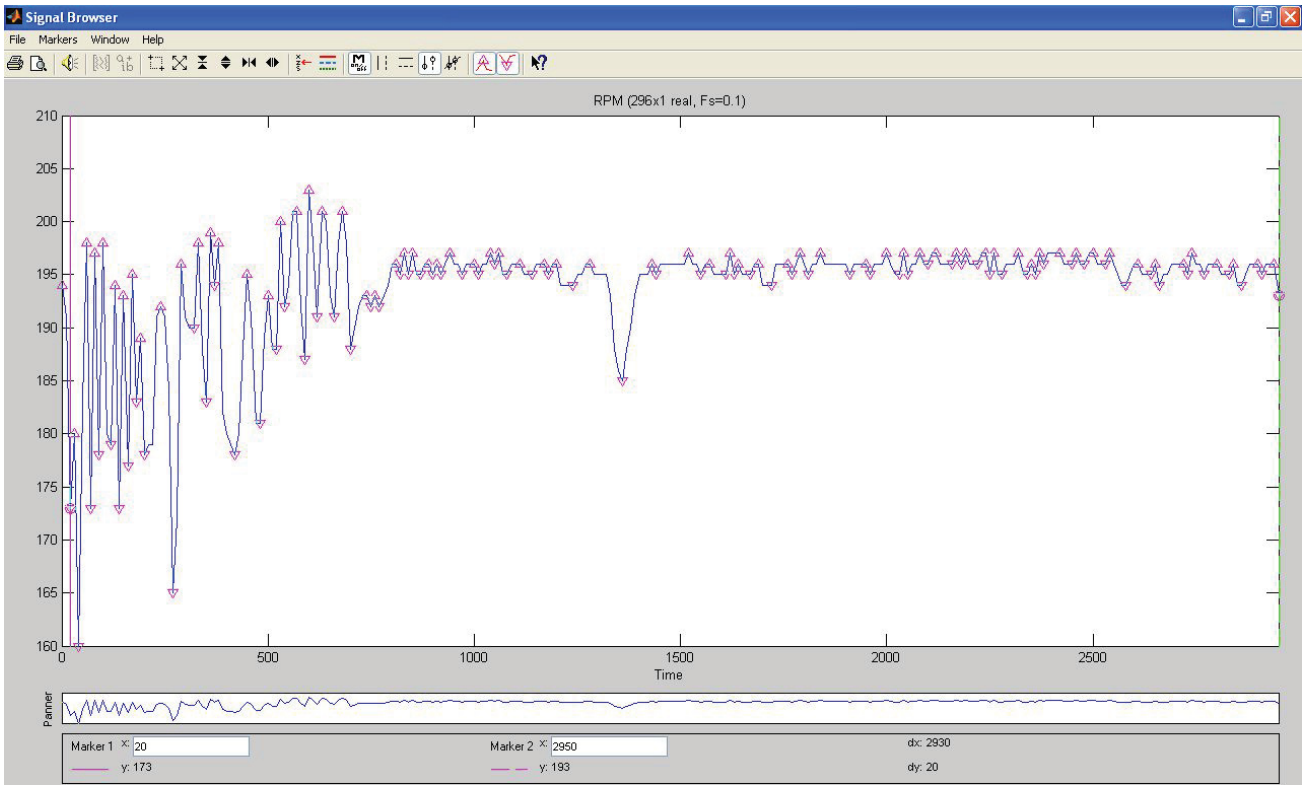

Figure 14 - Signal Browser with marked Peaks and Valleys

Using the peaks and valleys marked with the Signal Browser, the envelope curve can be obtained. The upper part of the envelope curve can be created by connecting the peaks which have been exported, the lower part of the curve by connecting the valleys.

The next step in order to calculate the stick-slip index is to determine the height of the envelope curve. This can be done by subtracting the values from the upper envelope curve from the values of the lower one. Unfortunately there are only values for the peaks and the valleys at the moment, but since a peak can not be at the same place like a valley, an interpolation has to be done in order to get the values of the opposite side of a peak or valley. The interpolation process can be done using a simple linear interpolation between two peaks or two valleys, using MATLAB's integrated interpolation function. Once each peak has its opposing data point, as well as each valley has its corresponding point on the upper envelope curve, the height of the envelope curve can be calculated.

Since the stick-slip index is calculated by dividing the height of the envelope by a running average, a running average of all the rpm values has to be determined. Again, a function already integrated in MATLAB can be used for this calculation step. A filtering function can be

adjusted to calculate a running average. For this thesis the values for rpm have been averaged over five data points, which is equal to one average value per 50 seconds of data. The filter function takes two values which are located before the point of investigation, two data points located after the point of interest, as well as the value of the point of interest itself. Due to this calculation procedure this function can not be used to run in real-time, because it is somehow “looking into the future”. The first few values of the running average are not useful because the function needs some values from the past to work properly, otherwise they will be set as zero, resulting in a lower running average than it should actually be.

After preparing all the necessary input parameters for the calculation of the stick-slip index, it can be calculated by the dividing the height of the envelope curve by the running average. The results can then be plotted.

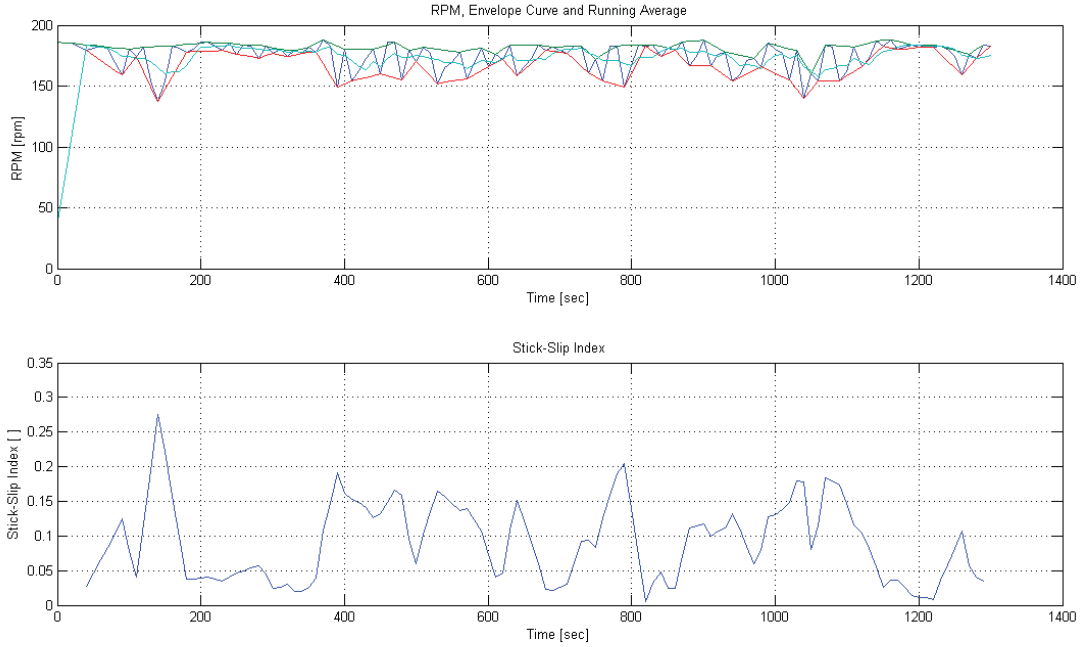

Figure 15 - Stick-Slip Index Calculation

As it can be seen in the plot above, the highest values of the stick-slip index can be found in the regions where the largest fluctuations of the rpm values occurred. This is due to the large height of the envelope curve in these regions.

Verification of the Results

The stick-slip index has been calculated and computed for several drilling intervals. In order to verify the results, the downhole magnetometer values showing the angular position of the measurment tool have been plotted for the same time ranges as the drilling intervals. If stick-slip has set in during drilling, a plot of the magnetometer values against the time should look similar to the pattern in figure 10 above. The sticking times of the drillstring should easily be detectible. By dividing the number of sticking phases by the amount of seconds in one plot, the stick-slip frequency can be determined. This frequency should be below 1 Hz, as mentioned earlier in the work.

Some sample results will be shown and discussed in the next paragraphs.

The first example shows the stick-slip index for an about 50 minute drilling interval. As it can be seen, the stick-slip index is rather high in the first 10 minutes, while the value is quite low for the rest of the drilling interval.

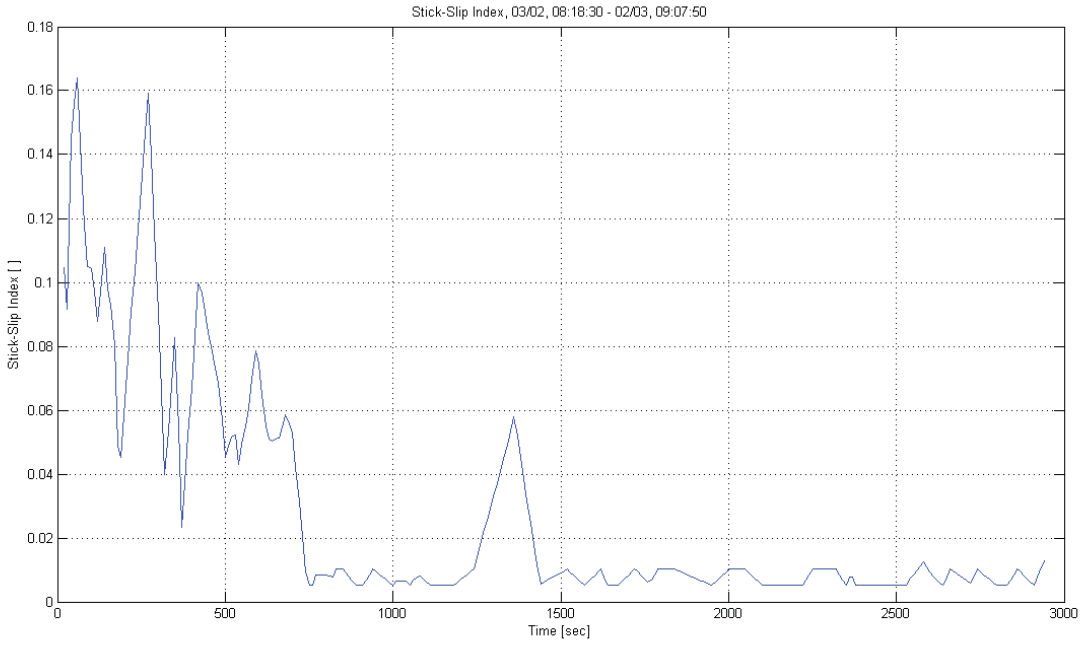

Figure 16 - Stick-Slip Index

Stick-slip can be expected in the first 10 minutes of the drilling interval, where the values are rather high when comparing them with the low values to follow. The next plot shows two plots of the magnetometer values recorded downhole. Each of the plots is covering a two minutes interval from the first ten minutes of drilling, where the high values for the stick-slip index were computed.

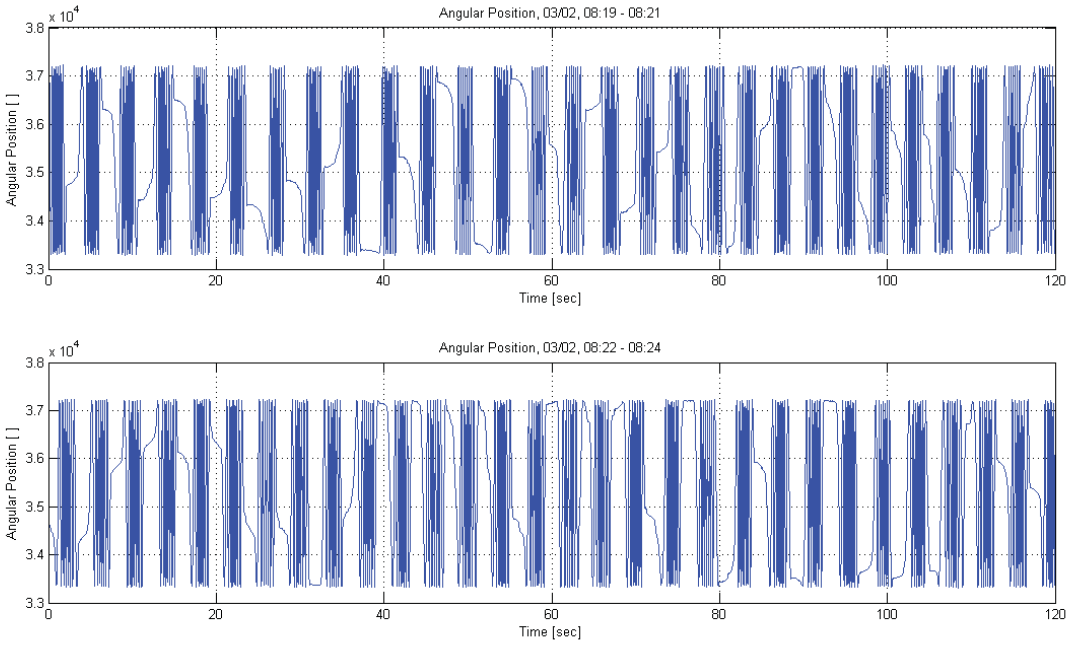

Figure 17 - Angular Position during Stick-Slip

As it can be depicted from the two plots above, there is no regular rotation of the drillstring, but it is alternately rotating and sticking. 28 sticking phases were recorded in the 120 seconds of the first plot, resulting in a stick-slip frequency of 0.23 Hz. The frequency is a little bit higher during the 120 seconds of the second plot, where 30 sticking phases were observed, resulting in a stick-slip frequency of 0.25 Hz.

On the other hand, when taking two examples showing the magnetometer readings from two time points where the stick-slip index has a lower value, no sticking phase is detectable.

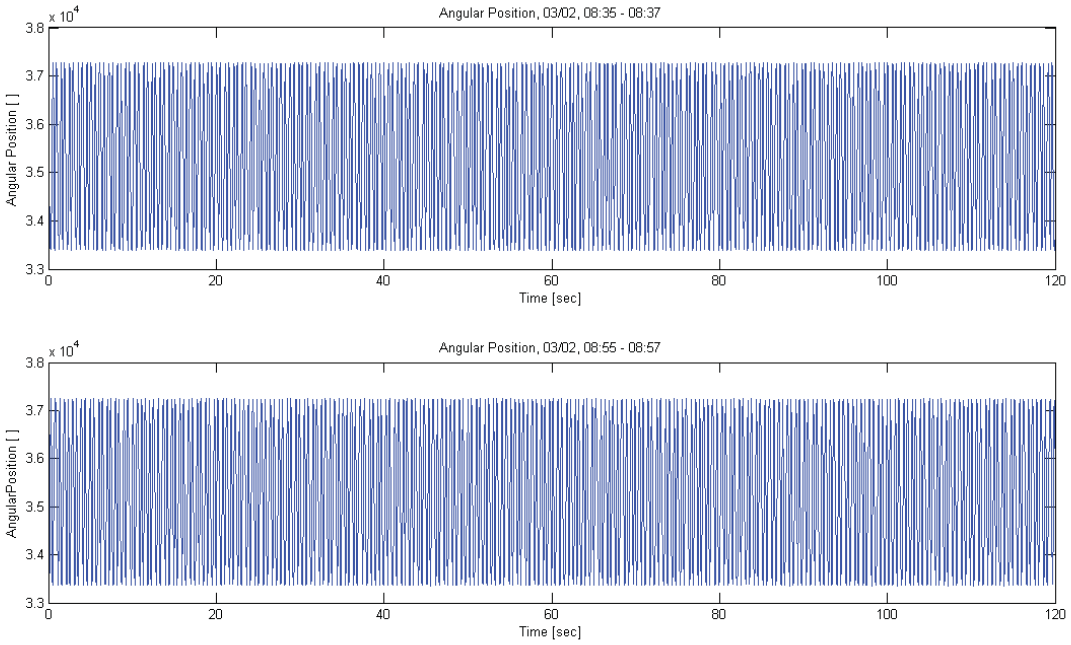

Figure 18 - Angular Position during Drilling

To verify the results, the same analysis should be done for another drilling interval. I chose to compute the results for a drilling interval from the same BHA run, not only because there were also high values of the stick-slip index, but also to prove the dependency of the stick-slip frequency on the drillstring. The next plot shows the stick-slip index for a drilling interval of about 70 minutes. The interval was drilled a little bit more than one hour after the drilling interval discussed before.

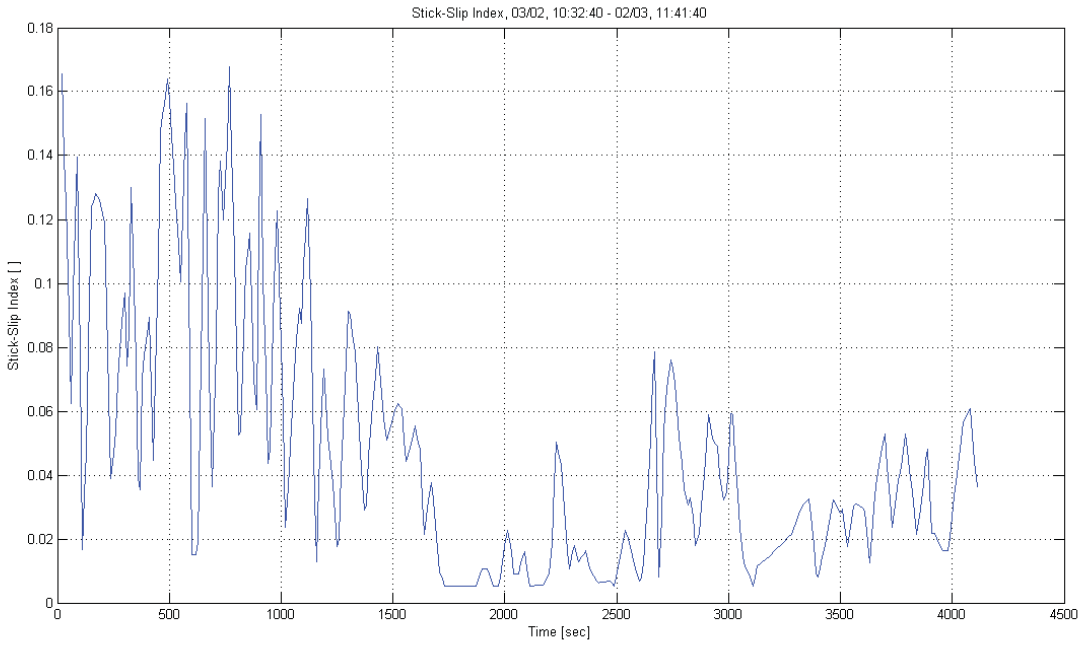

Figure 19 - Stick-Slip Index

Again, the highest values for the stick-slip index can be found in the first half of the drilling interval, here during the first 20 to 30 minutes. Stick-slip could be expected in this region. To verify the forecast, the magnetometer values have been plotted for one time point from the first 30 minutes, and for one time point from little peak at the beginning of the second half of the interval.

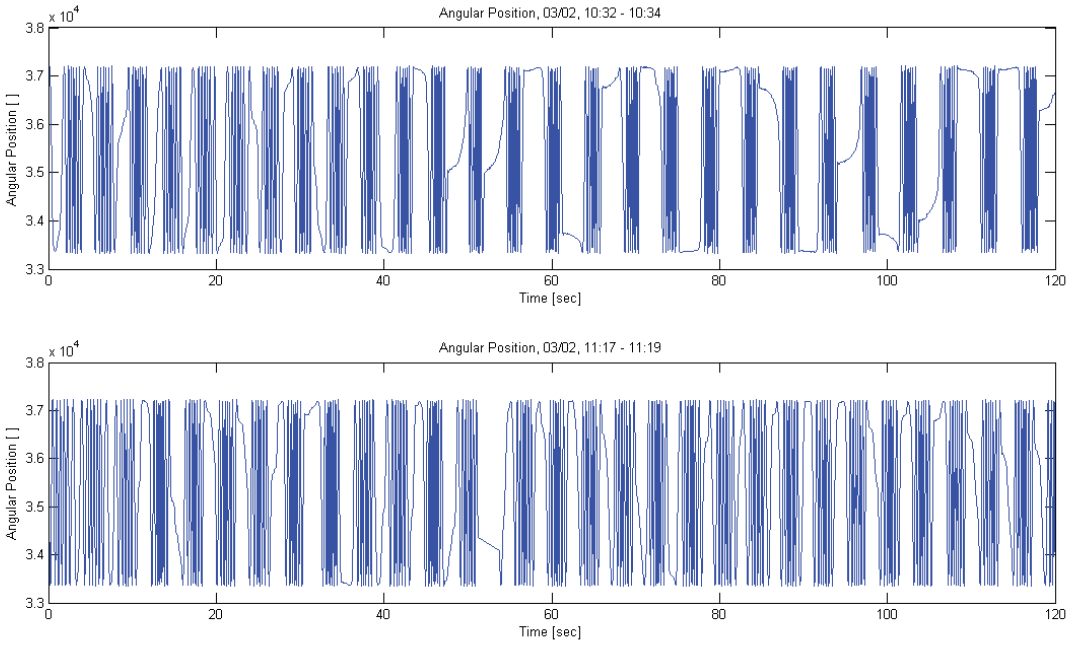

Figure 20 - Angular Position during Stick-Slip

As shown in the first graph of the plot, 28 sticking phases were recorded in the two minutes drilling interval. This corresponds to a stick-slip frequency of 0.23 Hz. The second graph is taken from the section where the stick-slip index is a little bit lower, but still high enough to show stick-slip behaviour. The first few seconds show indications of stick-slip behaviour, as the bit is rotating at different speeds. Two phases of slow rotation can already be seen. Afterwards the stick-slip motion sets in. The gap in the middle looks at fist sight like a longer sticking phase, but it is because of one of the recording stops which occurred after every 10 minutes. Therefore no data points are there. It can be assumed that one slipping phase is missing in this gap. Also taking the two periods of slow rotation at the beginning of the two minute interval into account, there are 30 sticking phases in total in the interval, resulting in a stick-slip frequency of 0.25 Hz.

It has been proved with these examples from the same BHA run, that the stick-slip frequency is only dependent on the drillstring once it had set in. The other influencing parameters like formation or bit do not play a role any more. Furthermore it has been proved by these examples that the calculation of the stick-slip index is able to deliver reasonable forecasts that stick-slip conditions have developed.

Influence of Stick-Slip on other Parameters

Once stick-slip has developed, other parameters change their behaviour, too. The values for hookload start variying, as well as the values for torque. The different parameters measured downhole by the measurement tool also show different patterns than they normally do.

Surface Parameters

The fluctuating values of the RPM measurement have been used for the detection of stick-slip. Nevertheless there are other parameters at surface that show different behaviour.

A comparison of plots of stick-slip index with plots of hookload indicates that the hookload is higher under stick-slip conditions than under normal drilling conditions. Furthermore the values of hookload show greater fluctuations than they normally do. This may be because of the uncontrolled force transfer due to the sudden changes between static and kinetic friction.

The first example shows a plot of stick-slip index against the time, as well as a plot of hookload versus time. The drilling interval that was chosen was the same as the first one for the discussion of the forecast results.

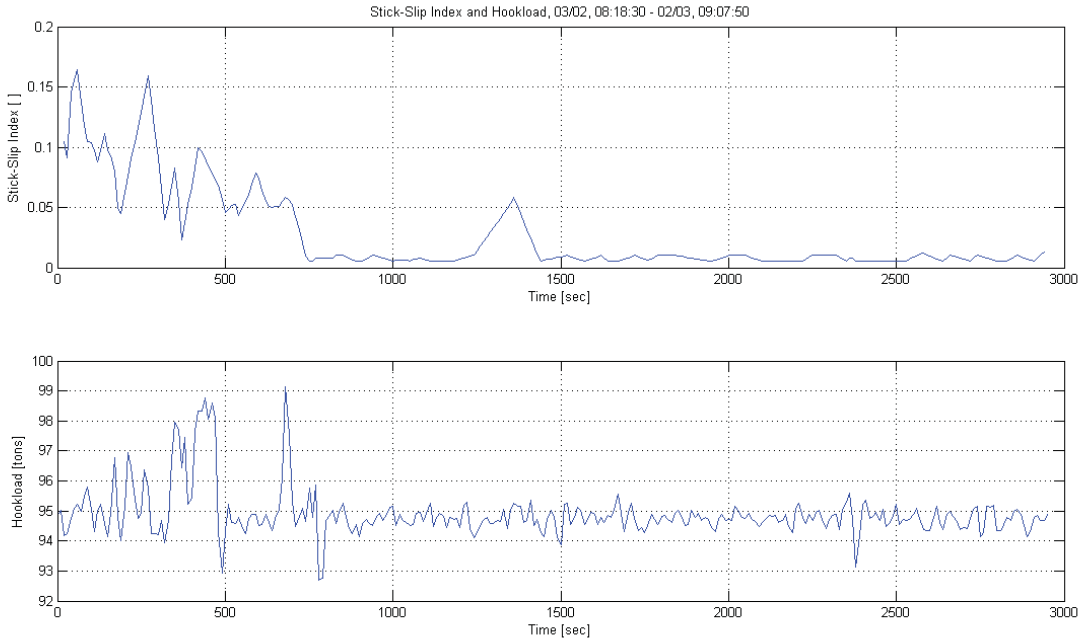

The hookload remains quite stable in the areas of low stick-slip index. In the regions where the stick-slip index has high values, the hookload values are also considerable higher. The fluctuation of the values is also higher than in the areas of low stick-slip index.

A second example, taken from the same BHA run one and a half hour later, shows the same tendencies:

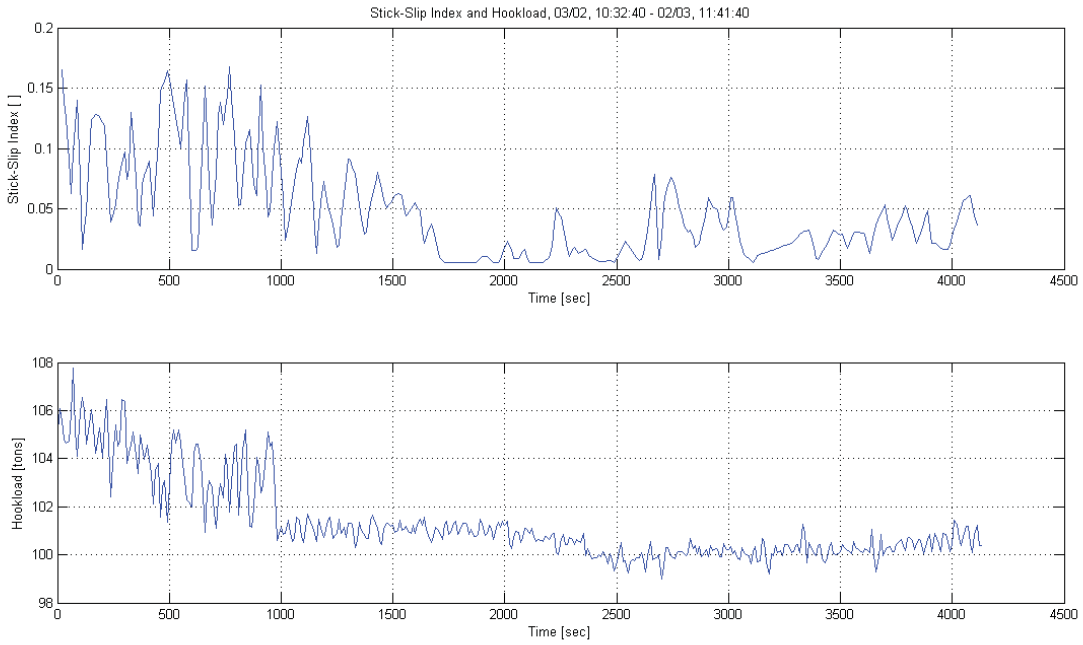

Figure 21 - Stick-Slip Index and Hookload

Again, it is easy to see that the hookload is higher in the areas of high stick-slip index. And, as in the example before, the values are not as constant as they are in the regions of low stick-slip index.

Another surface parameter that has been investigated is the torque. It can be assumed that the torque during drilling in stick-slip conditions is higher than during drilling in normal conditions because a higher torque will be required to overcome the static friction during the sticking phases.

Plots of stick-slip index and torque will be used to verify this assumption. The examples have been taken from the same drilling intervals as for the verification of the stick-slip forecasts and the effects of stick-slip on the hookload values.

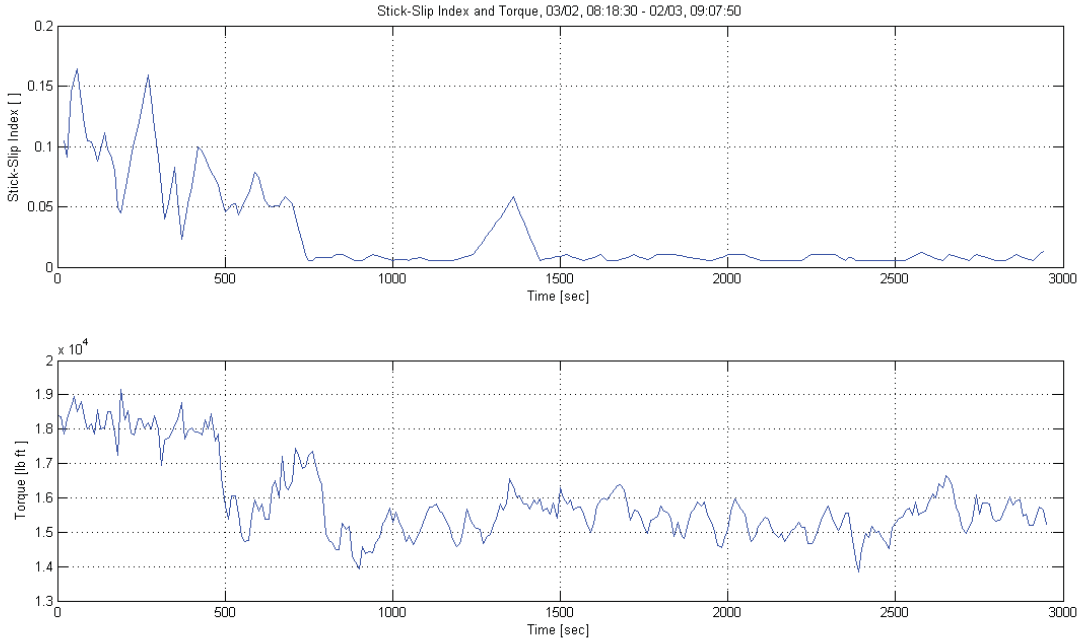

Figure 22 - Stick-Slip Index and Torque

Similar to the hookload values the torque values are higher in the regions of high stick-slip index than in the regions of low index. Fluctuations of the values can be found in both regions, regardless of the stick-slip index.

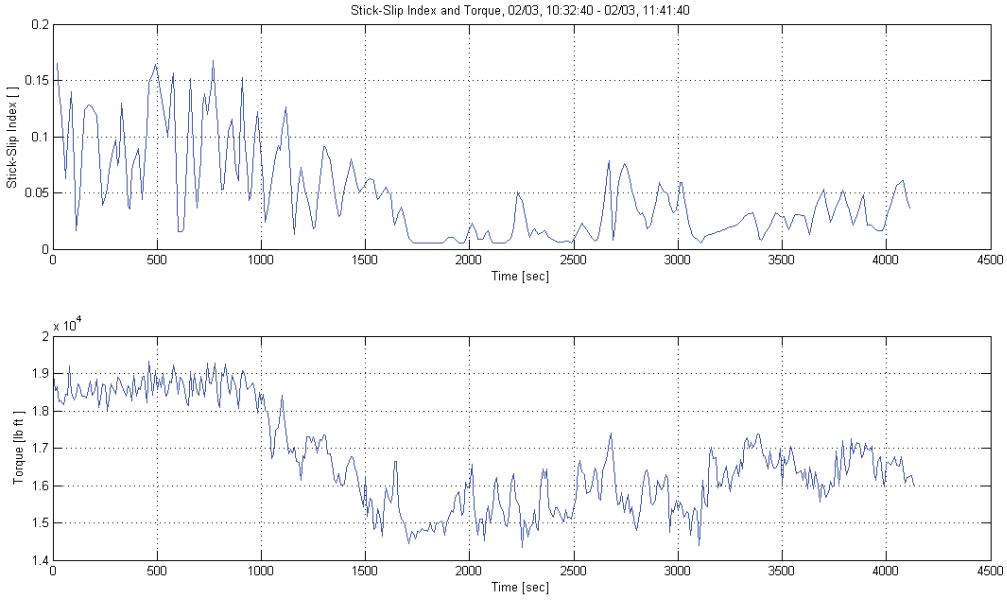

The second example, taken from the same BHA run one and a half hours after the first example, again proves that the torque measured at surface is higher in the regions of high stick-slip index. The fluctuations seem to be higher in the areas of low stick-slip index, which is rather strange because it is totally different to the facts that can be found in the literature. Since only one data set was supplied for this thesis, it is impossible to draw a conclusion what causes these fluctuations.

Downhole Parameters

Similar to the surface parameters, the downhole parameters exhibit abnormal behaviour during stick-slip. During the slip phase, when the pipe starts rotating again, very high accelerations can be detected. These accelerations may be damaging to the downhole equipment, as they can reach values of several times the gravitational acceleration.

The lateral accelerations are recorded with the downhole tool by the means of four sensors, placed with 90° spacing.

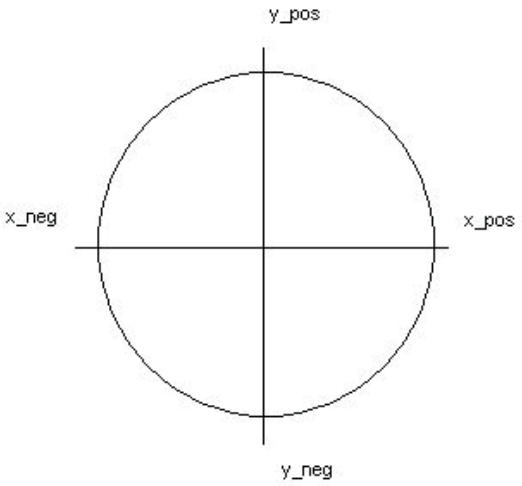

Figure 23 - Lateral Accelerometers

The resultant accelerations in X and Y direction can be obtained by adding the corresponding accelerations:

$$X = X\_pos + (-1)X\_neg \quad \text{Eq. 49}$$

$$Y = Y\_pos + (-1)Y\_neg \quad \text{Eq. 50}$$

X……...Resultant acceleration in X-direction [g]
Y……...Resultant acceleration in Y-direction [g]
X_pos..Acceleration in positive X-direction [g]
X_neg..Acceleration in negative X-direction [g]
Y_pos..Acceleration in positive Y-direction [g]
Y_neg..Acceleration in negative Y-direction [g]

In an inclined borehole the influence of the gravitational acceleration is clearly detectable, as it is measured twice during each rotation:

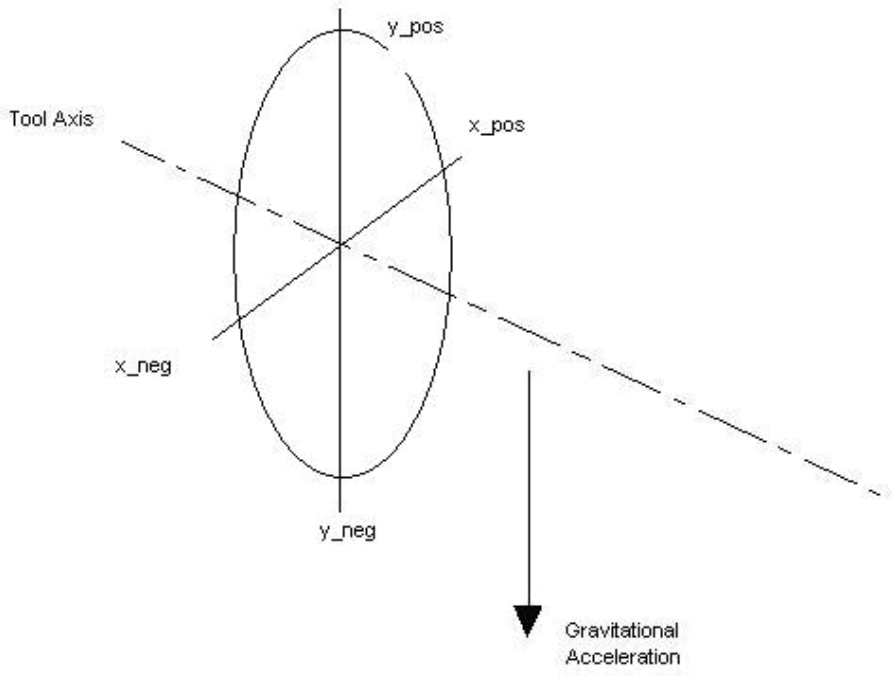

Figure 24 - Influence of Gravitational Acceleration

This can also clearly be seen on a filtered plot during drilling. On the following picture the high frequency contents of the signal have been removed by using a low-pass filter. The circular shape in the acceleration plot is due to the gravitational acceleration. In a vertical well none of the sensors would measure the gravitational acceleration. Therefore the ideal plot in a vertical well would only be a point in the middle. On the other hand, a horizontal well would have a radius of 1 [g] on the accelerations plot, as the whole gravitational force would be measured twice by the sensors during each rotation. The radius of the circle in the accelerations plot is equal to the sine of the inclination.

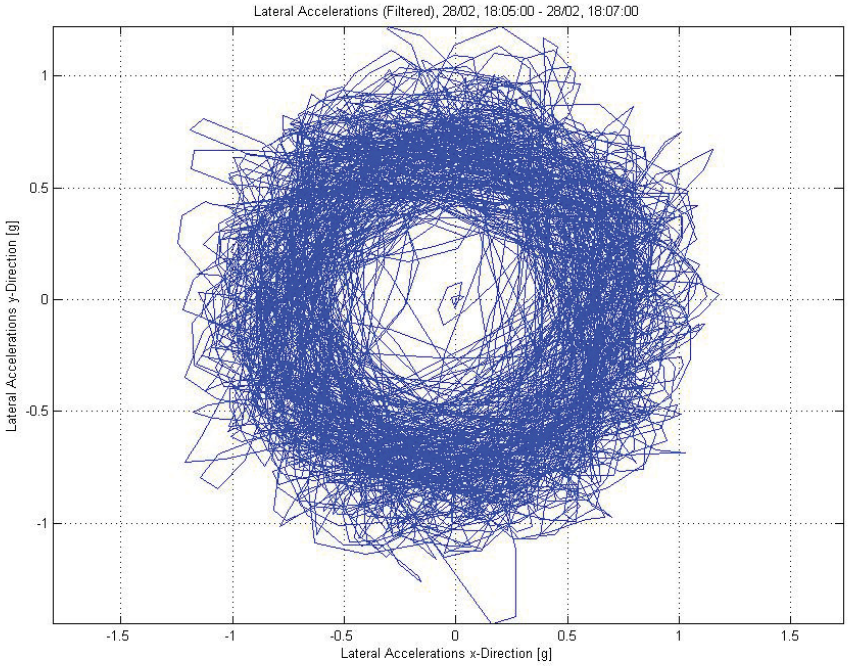

Figure 25 - Lateral Acceleration during Drilling, Filtered

In the unfiltered image the circular shape is not visible that clearly:

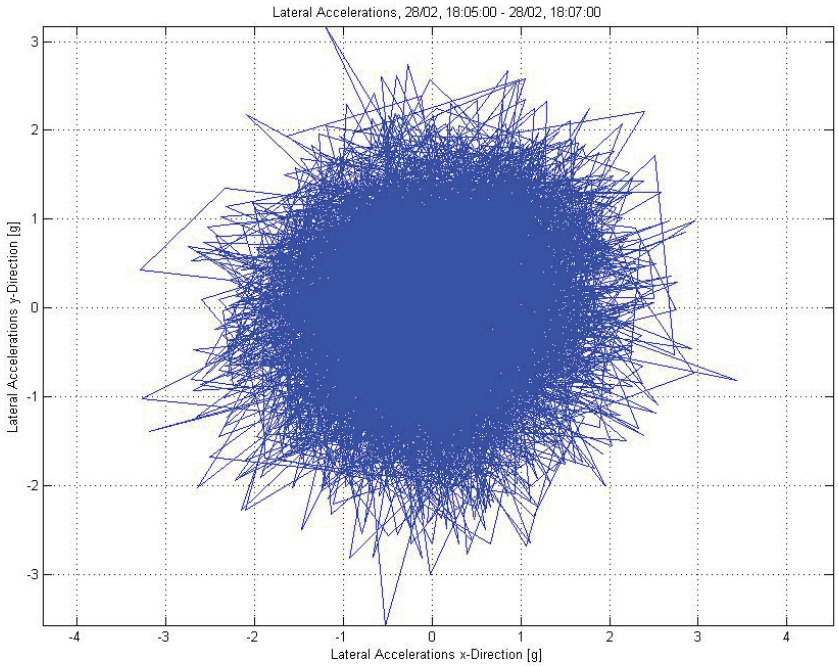

Figure 26 - Lateral Acceleration during Drilling, Unfiltered

As it can be seen in the unfiltered image, even during normal drilling there are shock loads present, but these shock loads never reach very high values and they are also not very oriented, so that no special part of the equipment is subject to shock loads all the time. During stick-slip conditions the shock loads reach much higher values, and they also show some kind of orientation. This means that the same parts of the equipment have to cope with the shock loads over and over again, which might be damaging to the equipment.

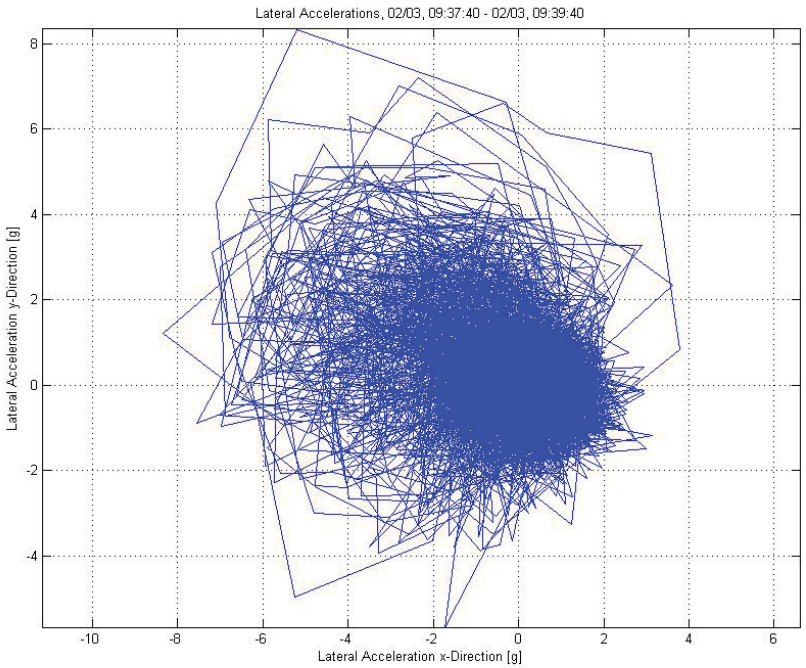

Figure 27 - Lateral Acceleration during Drilling in Stick-Slip Conditions, Unfiltered

On the picture above it can be seen that accelerations reach over 8 times the gravitational acceleration. Furthermore an orientation of the shock loads can be detected. The circular shape which is due to the rotation and the gravitation can be found in the lower right part of the plot. A filtered image shows this circular shape more clearly (note that the scale changed when comparing with the upper image).

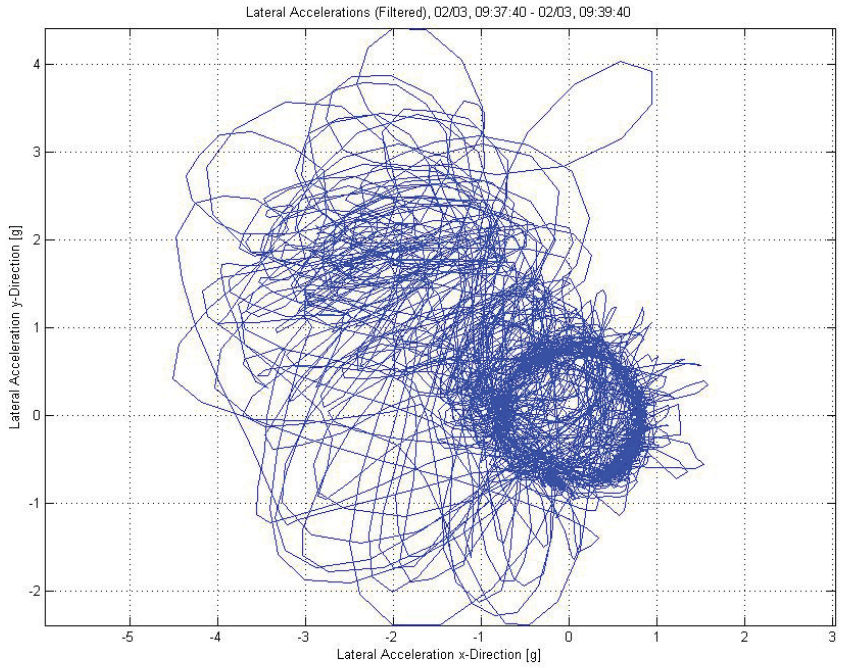

Figure 28 - Lateral Acceleration during Drilling in Stick-Slip Conditions, Filtered

The weird elliptical shapes on the plot might be because of the very fast pipe rotation at the beginning of the slip phase during stick-slip.

Outlook

Neural Networks

General

Neural networks are computer systems which are modelled similar to the human brain. A neural network consists of several interconnected processing elements (neurons). Each of these basic processing elements may have several inputs and one output. Two or more neurons may be combined in a layer. A neural network may consist of several layers. The layer which produces the output is called output layer, while the other layers are hidden layers.

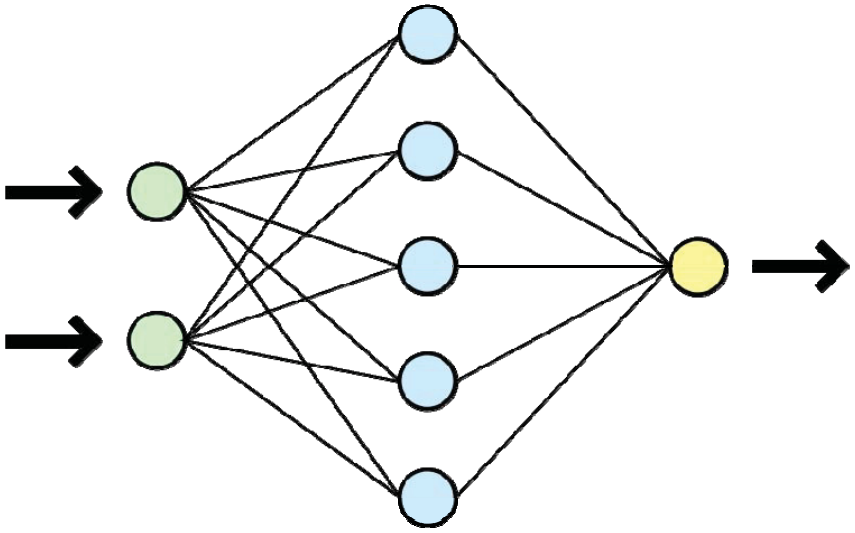

Figure 29 - Neural Network composed of 3 layers

The output of a single neuron is determined by the following formula [11]:

$$a = f\left(\overline{w}^{T} \cdot \overline{p} + b\right) \qquad \text{Eq. 51}$$

$\overline{w}$…….. Weight vector

p…….. Input vector

a…….. Output vector

b…….. Bias
f…… Activation function

A layer has a weight matrix, similar to the weight vector used for the neuron, as well as a bias vector and an output vector. The output from each intermediate layer is used as input to the following layer.

Training of Neural Networks

In order to perform their task neural networks have to be trained. This is done by using a set of input data and correct output data. The neural network produces its own output data after feed with the input data. This output has to be compared with the target output data. If there are any differences, then the weights and biases have to be modified.

After doing so, the output of a neural network has to be checked by using a so called test set. This is a set with known inputs and outputs which were not used for training purposes. With this test set the quality of the neural network can be checked by verifying how well the neural network can generalize.

One common problem during neural network training is overfitting. If the neural network is overfitted it remembers the training examples rather than learning to generalize to a new situation.

Conclusions

Axial force transfer can be simulated quite well by using spring-mass models. These models are capable of modelling the behaviour of the drillstring. The big advantage to simple torque and drag models is the incorporation of dimensional changes into the model. External forces acting on the drillstring change its dimensions. The drillstring can be in tension or in compression. Each of these modes can be modelled using a spring-mass model.

A spring-mass model is able to deliver more exact results than a common torque and drag model, even when neglecting the transient behaviour of the springs. When kept simple, the model might even be used in real-time applications, because it is not very demanding regarding computer performance.

The big advantage of a spring-mass model is its ability to model the behaviour of different drilling dysfunctions, like stick-slip. The increase of potential energy during the sticking phases, as well as its release during the slipping phases can be simulated with a spring-mass model.

In order to take full advantage of such a model, it has to be assured that the different drilling dysfunctions are detected in real-time. The detection of buckling is quite simple using the equations to calculate the critical buckling loads. The influence of buckling is an increase in friction, which influences the axial force transfer. Detecting stick-slip conditions is more difficult, but it can be detected by calculating a stick-slip index. As it has been proved in this paper, it is possible to detect stick-slip conditions with this index, even when using low frequency input data.

The determination of the friction factors in a wellbore is also essential for the use of a spring-mass model. There are two methods proposed in this paper, one for the calculation of an overall wellbore friction factor, and one for calculating an incremental friction factor. Applying these methods is not difficult and only hookload data, which are generally available at a drilling rig, and well survey data are needed for calculation.

Spring-mass models are made up of several segments. The more segments are used, the more exact the results will be, but the computer performance consumption increases, too. In order to run more exact calculations in real-time mode in the future, neural networks may be used. When getting well trained, the neural networks are applicable for a wide range of applications. Nevertheless, they can only be used in regions where they have been trained to. Spring-mass models may be used together with neural networks then, in order to deliver data which can be used as training input data for neural networks.

List of References

1. Paslay, P.R., ”Stress Analysis in Drillstrings”, SPE 27976 presented at the 1994 University of Tulsa Centennial Petroleum Engineering Symposium, Tulsa, Aug. 29-31
2. Reiber, F., Vos, B.E., Eide, S.E., “On-Line Torque & Drag: A Real-Time Drilling Performance Optimization Tool”, SPE 52836 presented at the 1999 SPE/IADC Drilling Conference, Amsterdam, March 9-11
3. Cardoso, J.V., Maidla, E.E., Idagawa, L.S.,”Problem Detection During Tripping Operations in Horizontal and Directional Wells”, SPE 26330 presented at the 1991 SPE Annual Technical Conference and Exhibition, Houston, October 3-6
4. He, X., Sangesland, S., Halsey, G.W.,”An Integrated Three-Dimensional Wellstring Analysis Program”, SPE 22316 presented at the 1991 Sixth SPE Petroleum Computer Conference, Dallas, June 17-20
5. Desmette, S., Will, J., Coudyzer, C., Richard, T., Le, P., “Isubs: A New Generation of Autonomous Instrumented Downhole Tool”, SPE 92424 presented at the 2005 SPE/IADC Drilling Conference, Amsterdam, February 23-25
6. Kuru, E., Martinez, A., Miska, S., Qiu, W., “The Buckling Behaviour of Pipes and Ist Influence on Axial Force Transfer in Directional Wells“, SPE/IADC 52840 presented at the 1999 SPE/IADC Drilling Conference, Amsterdam, March 9-11
7. Hishida, H., Ueno, M., Higuchi, K., Hatakayama, T., “Prediction of Helical / Sinusoidal Buckling“, IADC/SPE 36384 presented at the 1996 IADC/SPE Asia Pacific Drilling Technology Conference, Kuala Lumpur, September 9-11
8. Pavone, D.R., Desplans, J.P., “Application of High Sampling Rate Downhole Measurements for Analysis and Cure of Stick-Slip in Drilling”, SPE 28324 presented at the 1994 SPE 69th Annual Technical Conference and Exhibition, New Orleans, September 25-28
9. Dufeyte, M-P., Henneuse, H., “Detection and Monitoring of the Stick-Slip Motion: Field Experiments”, SPE/IADC 21945 presented at the 1991 SPE/IADC Drilling Conference, Amsterdam, March 11-14
10. Chen, S.L., Blackwood, K., Lamine, E., “Field Investigation of the Effects of Stick-Slip, Lateral, and Whirl Vibrations on Roller-Cone Bit Performance”, SPE 76811 revised from SPE 56439, first presented at the 1999 SPE Annual Technical Conference and Exhibition, Houston, October 3-6
11. Dashevskiy, D., Dubinsky, V., Macpherson, J.D., “Application of Neural Networks for Predictive Control in Drilling Dynamics”, SPE 56442 presented at the 1999 Annual Technical Conference and Exhibition, Houston, October 3-6